Journal of Structural Geology, Vol. 6, No. 5, pp. 477 to 497, 1984
Printed in Great Britain

0191-8141/84 $03.00 + 0.00

Strain path partitioning within thrust sheets: microstructural and petrofabric evidence from the Moine Thrust zone at Loch Eriboll, northwest Scotland

R. D. LAW, R. J. KNIPE

Department of Earth Sciences, The University, Leeds LS2 9JT, U.K.

and

H. DAYAN

Universidade Federal do Rio de Janeiro, Instituto de Geociências Depto de Geologica, Ilhao do Fundão, CEP 21.910, Rio de Janeiro, Brasil

Abstract—Quartz *c* axis fabrics and microstructures have been investigated within a suite of quartzites collected from the Loch Eriboll area of the Moine Thrust zone and are used to interpret the detailed processes involved in fabric evolution. The intensity of quartz *c* axis fabrics is directly proportional to the calculated strain magnitude. A correlation is also established between the pattern of *c* axis fabrics and the calculated strain symmetry.

Two kinematic domains are recognized within one of the studied thrust sheets which outcrops immediately beneath the Moine Thrust. Within the upper and central levels of the thrust sheet coaxial deformation is indicated by conjugate, mutually interfering shear bands, globular low strain detrital quartz grains whose *c* axes are aligned sub-parallel to the principal finite shortening direction (*Z*) and quartz *c* axis fabrics which are symmetric (both in terms of skeletal outline and intensity distribution) with respect to mylonitic foliation and lineation. Non-coaxial deformation is indicated within the more intensely deformed and recrystallized quartzites located near the base of the thrust sheet by single sets of shear bands and *c* axis fabrics which are asymmetric with respect to foliation and lineation.

Tectonic models offering possible explanations for the presence of kinematic (strain path) domains within thrust sheets are considered.

INTRODUCTION

IN RECENT years considerable attention has been paid to the geometrical properties of thrust belts using the 'thin-skinned' model of thrust belt evolution proposed by Dahlstrom (1970). This model has been applied to the Moine Thrust zone (Fig. 1) of NW Scotland (Elliott & Johnson 1980, McClay & Coward 1981, Soper & Barber 1982, Butler 1982a) where a general WNW sequence of thrust propagation towards the foreland has been demonstrated. Thus structurally higher, more easterly outcropping thrusts are generally cut or folded by lower structures.

These geometrical studies provide an important foundation for more detailed analysis of deformation processes which operate during thrusting. For example, detailed studies of the deformation textures and fabrics generated during thrusting allow an insight into the conditions of deformation and the evolution of strains, together with an assessment of the rates and mechanisms involved in straining during thrusting (Schmid 1975, Elliott 1976). Such microstructural studies in the Moine Thrust zone (Christie 1963, Allison 1979, Dayan 1981, White *et al.* 1982) have demonstrated the importance of dislocation-controlled deformation mechanisms during thrusting and also facilitated the estimation of differential stresses associated with deformation (Weathers *et al.* 1979, White 1979, Dayan 1981).

This paper reports the results of microstructural and petrofabric analysis of deformation features developed in quartzites located to the east of Loch Eriboll at the northern end of the Moine Thrust zone of NW Scotland (Fig. 1). Field relationships in this area have been studied in detail by Soper & Wilkinson (1975), Coward (1980), McClay & Coward (1981) and Dayan (1981); the area therefore provides an excellent opportunity to study the deformation processes operating both within and at the base of thrust sheets.

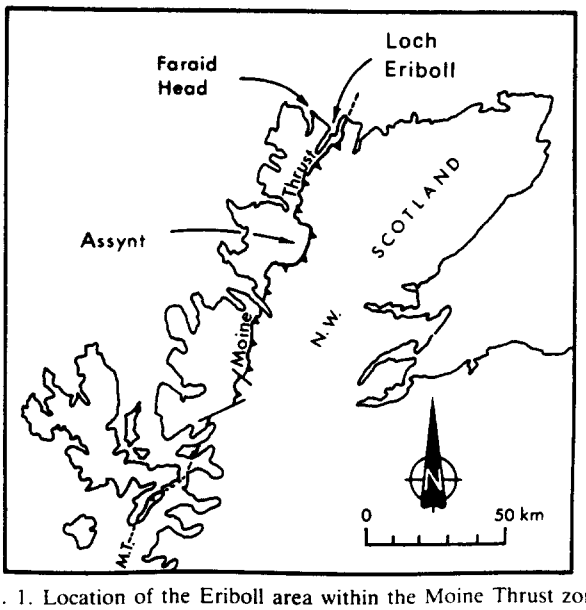

Fig. 1. Location of the Eriboll area within the Moine Thrust zone, Scotland.

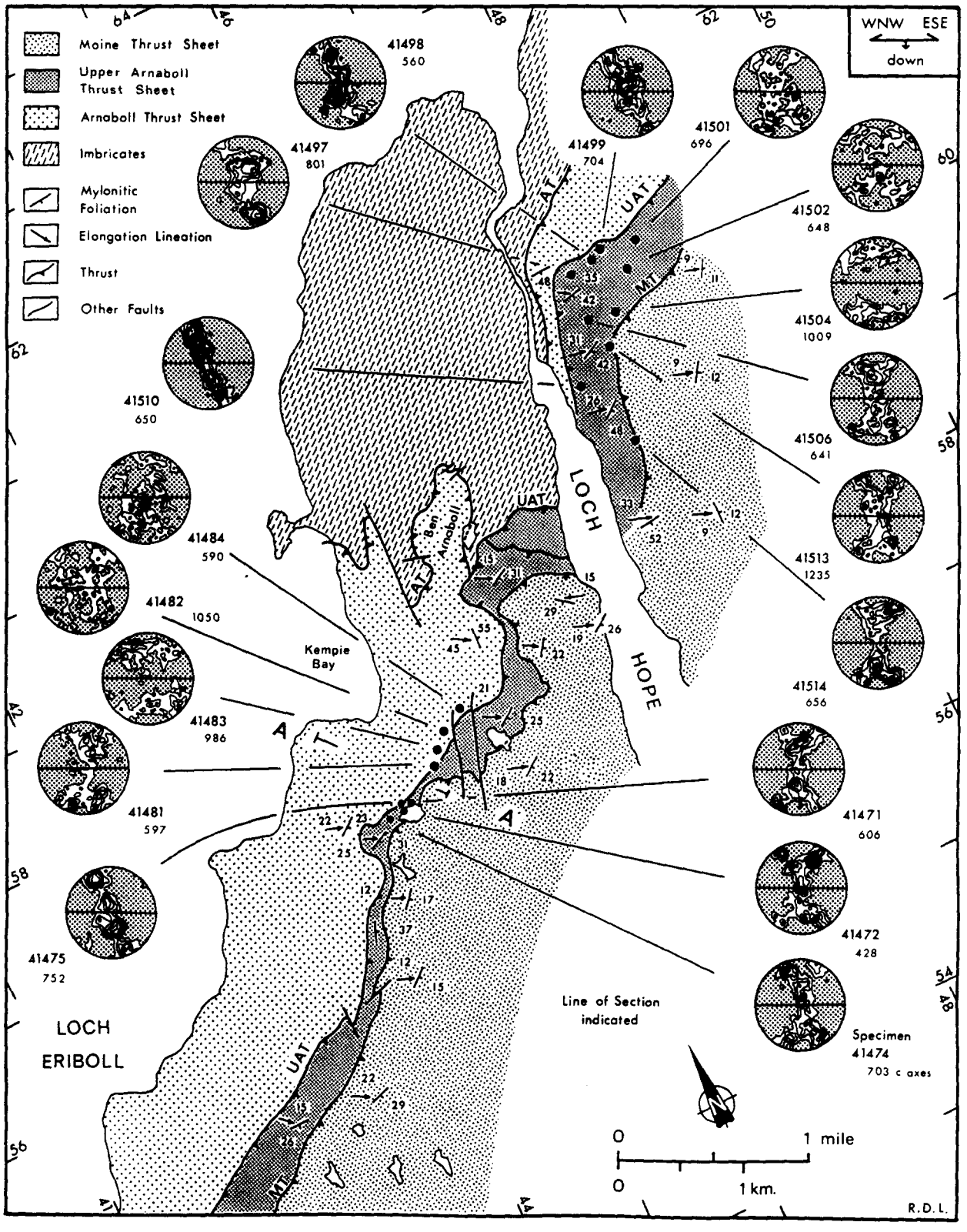

Fig. 2. Thrust sheets and quartz *c* axis fabrics of the Eriboll area. Location of specimens, line of cross-section (Fig. 3) and national grid coordinates indicated. AT, Arnaboll thrust; UAT, Upper Arnaboll thrust; MT, Moine thrust. Note that all stereograms are placed in a geographical reference frame and viewed towards the NNE. In this reference frame the ESE plunging grain-shape lineation lying within the foliation is represented as a horizontal structure. Specimen reference numbers and number of *c* axes measured in each specimen are indicated. Stereograms contoured by M. Casey at ETH, Zurich, using a modified version of the computer program described by Starkey (1970). Contour intervals: 1, 2, 3, . . . , 12 points per counting area, *c* axis free areas stippled. 0.2% counting area used for stereograms with less than 700 points; 0.1% counting area used for stereograms with 700 or more points.

THE STUDY AREA

Within the Eriboll area (Fig. 1) intensely deformed Proterozoic sediments (the Moine Schists) were thrust to the WNW over a foreland sequence of early Proterozoic Lewisian gneisses and Cambro-Ordovician sediments (for stratigraphic details see McClay & Coward 1981) during the Caledonian Orogeny (500–400 Ma).

Several thrust sheets, stacked one on top of the other and dipping gently to the ESE, are recognized in the Eriboll area (Fig. 2). The lowermost and most westerly thrust sheet contains an imbricated sequence of Cambro-Ordovician sediments; the base of this thrust sheet is termed the Sole Thrust (Peach *et al.* 1907). Structurally above these imbricates is the Arnaboll thrust sheet, consisting of Cambro-Ordovician sediments underlain by Lewisian gneiss. The contact between the Cambro-Ordovician and Lewisian rocks of the Arnaboll thrust sheet is considered to be of sedimentary origin. Structurally above the Arnaboll thrust sheet lies a sheet of intensely lineated and foliated mylonites (*L–S* tectonites) derived, primarily, from Cambrian quartzite and Lewisian gneiss. Because of the intense deformation it is uncertain if the contacts between the Lewisian and lenses of quartzite are of tectonic or sedimentary origin. Lying structurally above and to the east of this mylonite sheet are the Moine Schists.

The naming of the thrusts which form the upper and lower surfaces of this mylonite sheet have been the subject of some controversy. Study of the Geological Survey Memoir (Peach *et al.* 1907) and the accompanying one inch geological map (Sheet 114) suggests that the original Survey workers considered the base of the mylonite sheet to mark the position of the Moine thrust, the upper surface of the mylonite sheet being marked by an un-named thrust. However, as pointed out by Soper & Wilkinson (1975) more detailed study of the six inch Geological Survey maps of the area prepared by B. N. Peach and J. Horne indicates that the upper thrust (marking the contact between the mylonite sheet and the overlying Moines) was originally considered by these Survey workers to represent the position of the Moine Thrust. Along this fault line the word "Moine" in "Moine Thrust Plane" is clearly crossed out and initialled "B.N.P." On this map a lower thrust (corresponding in position to the lower surface of the mylonite sheet) is labelled "? MTP ?" and along this thrust trace there are always interrogation marks. Following the Survey geologists the lower and upper thrusts bounding the mylonite sheet are mapped as the Moine and Eriboll thrusts, respectively by Soper & Wilkinson (1975). Similarly, McClay & Coward (1981) mapped the base of these mylonitic rocks as the Moine thrust and consider the upper surface of the mylonite sheet to be marked by an un-named thrust. More recently, detailed mapping of the area has led Dayan (1981) to interpret the upper surface of the mylonite sheet as the Moine thrust. This re-interpretation is supported by Rathbone *et al.* (1983, fig. 2) who name the lower and upper surfaces of the mylonite sheet the Upper Arnaboll and Moine thrusts, respectively.

Following the terminology of Rathbone *et al.* (1983) this sheet of mylonitic Lewisian gneiss and Cambrian quartzite which rests on top of the less strongly deformed rocks of the Arnaboll thrust sheet will be referred to as the Upper Arnaboll thrust sheet in the present paper (Fig. 2).

Due to the absence of suitable off-set markers, the calculation of displacement along individual thrusts within the Moine Thrust zone has proved difficult. Butler (1982a) has suggested that total displacement within the Moine Thrust zone in the area immediately south of Loch Eriboll may be over 60 km. Displacement on the Moine Thrust (sensu stricto) is at least 11 km as Moine rocks outcrop (Fig. 1) at Faraid Head, Durness. However, as pointed out by Butler (1982a) some of this displacement may be taken up by movement on lower thrusts or duplex development.

Little detailed work has been done on the metamorphism of rocks within the Moine Thrust zone. An unpublished thermal index estimate of 3.7 made on dispersed palynomorphs from Fucoid Beds (see Fig. 3 for stratigraphic position) lying beneath the Moine Thrust in the Eriboll area by C. Downie (quoted in Soper & Barber, 1982; p. 134) indicates a temperature of approximately 200°C. Within the Moine Schists of the Eriboll area, greenschist-facies metamorphism is indicated by the growth of chlorite and white mica.

SPECIMEN LOCATION

The quartzite specimens described in this paper were collected from two adjacent thrust sheets outcropping to the east of Loch Eriboll. The first suite of specimens was taken from the Basal Quartzite (see Fig. 3 for stratigraphic position) which rests on top of unmylonitized Lewisian gneiss within the Arnaboll thrust sheet (Figs. 2 and 3) to the east of Kempie Bay. The second suite of specimens was collected from quartzites lying within mylonitised Lewisian of the adjacent, but structurally higher, Upper Arnaboll thrust sheet. Two areas were sampled within the Upper Arnaboll thrust sheet (Fig. 2): the first is located immediately to the east of the Arnaboll thrust sheet sampling area, the second being to the east of Loch Hope.

STRAIN AND PETROFABRIC ANALYSIS TECHNIQUES

The plastically deformed detrital quartz grains observed in these specimens have been used by Dayan (1981) as strain markers. Three mutually perpendicular thin sections were prepared from each specimen, and the orientation and aspect ratio of an average of one hundred and ten detrital quartz grains measured in each section. Various two and three-dimensional strain analysis techniques were then applied to this basic data.

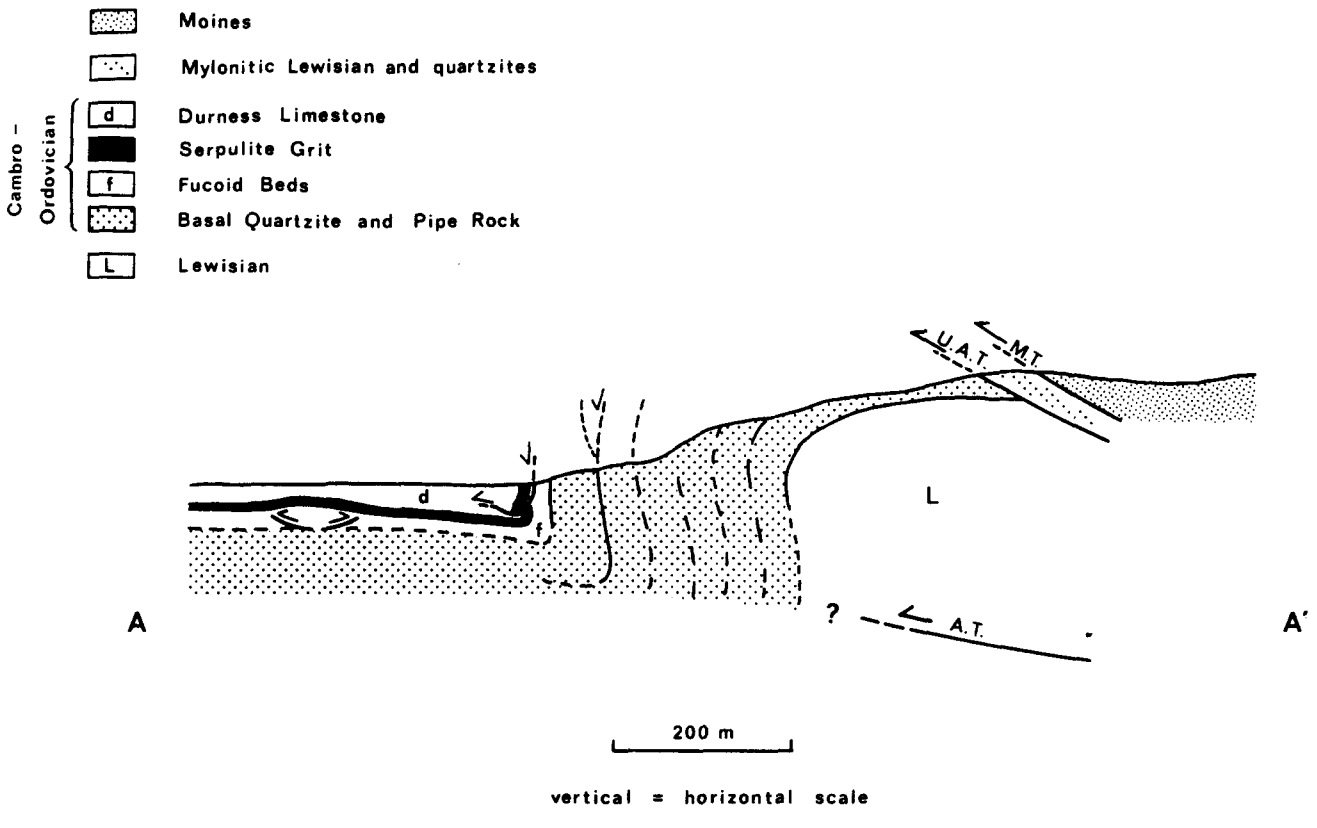

Fig. 3. Cross-section, viewed towards the NNE, through the Moine Thrust zone at Kempie Bay. Line of section indicated in Fig. 2. A.T., Arnaboll Thrust; U.A.T., Upper Arnaboll Thrust; M.T., Moine Thrust.

In this paper only the three-dimensional strain estimates (Fig. 4) indicated by program PASE 5 of Dunnet (1969) with input data by programme THETA (Peach & Lisle 1979) are quoted.

Strain analyses were not attempted on specimens in which recrystallization was considered to have significantly modified the aspect ratio of the observed detrital grains.

It must be emphasized that almost all thin sections were cut oblique to any observed foliation or lineation in the individual specimen. No assumptions concerning the possible relationships between foliation, lineation and the finite strain ellipsoid were made during the strain analyses carried out by Dayan (1981). Within observational error, however, it was always found that the X axis and XY plane of the calculated finite strain ellipsoid were orientated parallel to the specimen lineation and mylonitic foliation, respectively.

Petrofabric analysis of quartz c axis preferred orientation was carried out on one thin section from each specimen, using an optical microscope and universal stage, a minimum of 600 c axes being measured in each thin section. During petrofabric work on each specimen a record was kept of each grain measured, by plotting the sites of individual c axis measurements on an enlarged photograph of the thin section. This technique was found to be particularly useful when checking for domainal c axis fabrics.

The c axis data are displayed on equal-area, lower hemisphere stereographic projections whose plane of projection is the XZ principal plane of the calculated

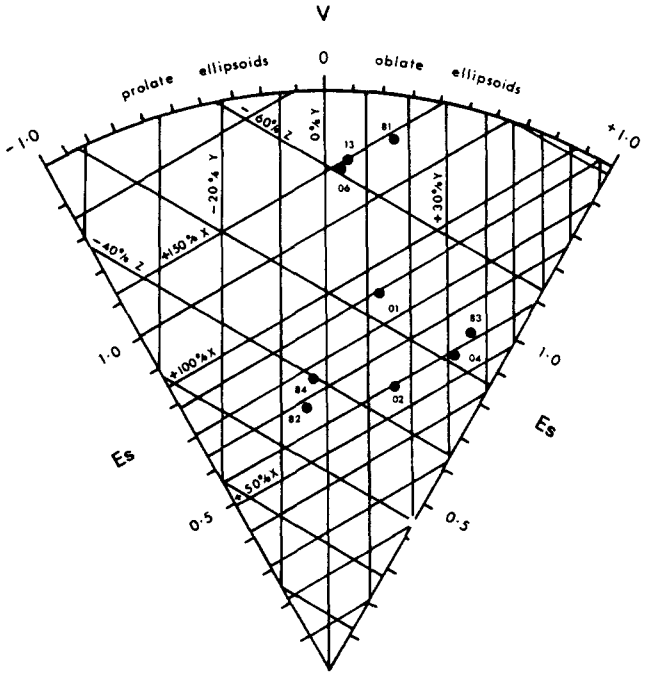

Fig. 4. Hsu natural strain plot of calculated strain states within the Arnaboll and Upper Arnaboll thrust sheets, specimens 41481–41484 being from the Arnaboll thrust sheet. Data taken from Dayan (1981). Elongations parallel to principal axes of the finite strain ellipsoid indicated. Es is natural logarithmic octahedral strain; Lodes ratio $V = (1 - k)/(1 + k)$.

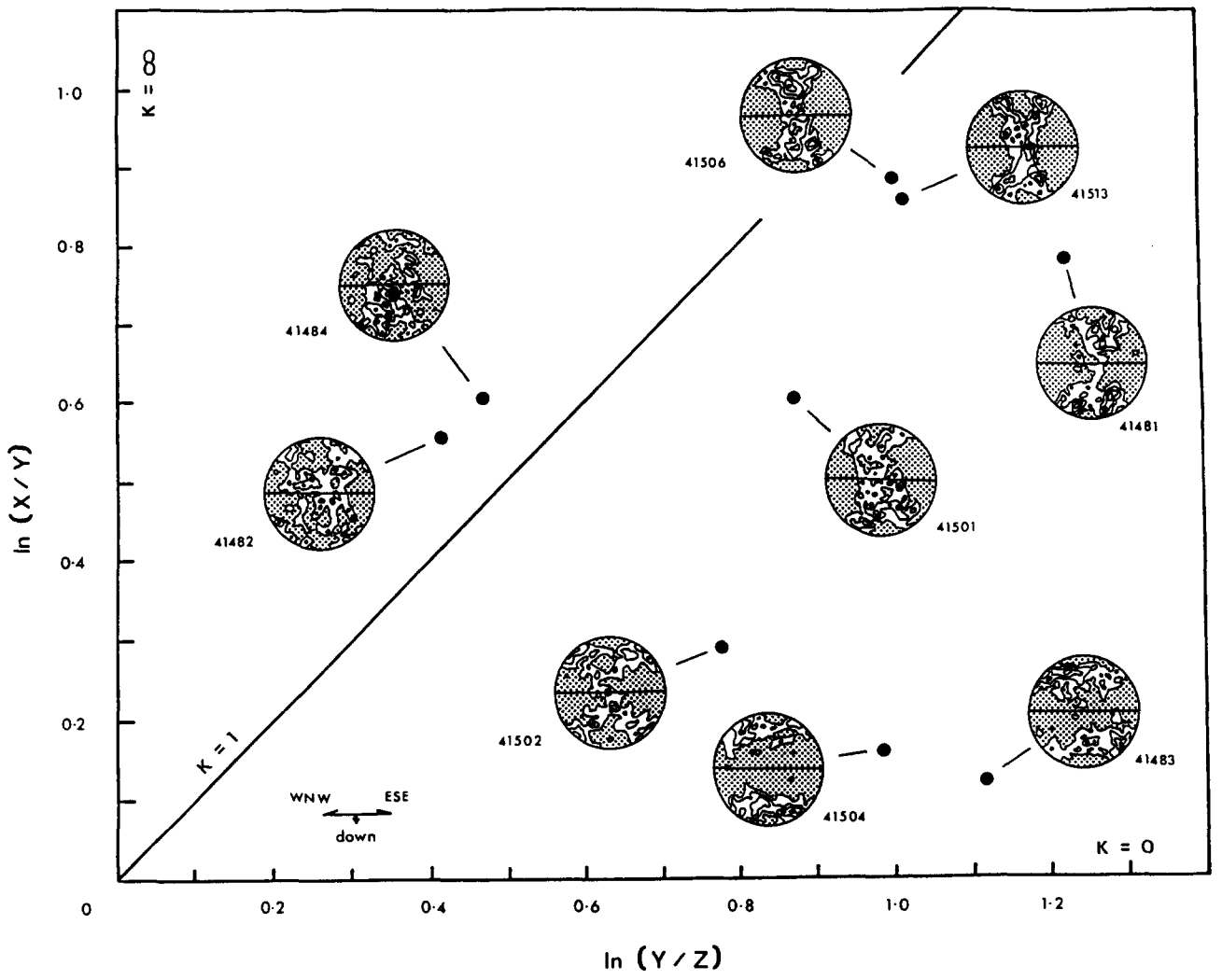

Fig. 5. Natural log. Flinn plot illustrating relationships between *c* axis fabrics of detrital quartz grains and calculated strain states within the Arnaboll and Upper Arnaboll thrust sheets. *X*, *Y* and *Z* are maximum, intermediate and minimum principal axes of the calculated finite strain ellipsoid, respectively. In each stereogram the calculated *XY* plane is vertical, and *X* horizontal. Strain analysis data taken from Dayan (1981). Geographical orientation of stereograms indicated. For explanation of contour intervals see Fig. 2.

strain ellipsoid. In specimens where recrystallisation had become too advanced for strain analysis to be attempted, *c* axes were rotated into a specimen reference frame represented by an equal-area lower-hemisphere projection in which the foliation was vertical and lineation within the foliation was horizontal. In geographical terms all of these stereograms are viewed towards the NNE, the calculated ESE plunging *X* axis (lineation) being represented as a horizontal structure. *C* axis plots were contoured by M. Casey at E.T.H., Zurich using a modified version of the computer program developed by Starkey (1970).

Observed relationships within the Arnaboll and Upper Arnaboll thrust sheets between *c* axis fabrics of detrital quartz grains and the calculated strain ellipsoid are shown in Fig. 5. Within both thrust sheets specimens with calculated flattening strains display *c* axes which lie on a small-circle girdle (opening angle 30–45°) about *Z*. For specimens that indicate approximate plane strain, a cross-girdle fabric was detected, consisting of a small-circle girdle (of similar opening angle) about *Z* and connected through *Y*.

FABRIC DEVELOPMENT WITHIN THE ARNABOLL THRUST SHEET

Microstructure and strain analysis of quartzites within the Arnaboll thrust sheet

The least deformed specimens in this study were collected (Figs. 2 and 6) at a vertical distance of approximately 60–80 m below the Upper Arnaboll thrust. Detrital quartz grains possess length–width ratios of less than 3:1 in approximate *XZ* sections, and display a preferred orientation of clast long axes (Fig. 7a). Undulose extinction and poorly defined deformation bands are observed within the detrital grains. Minor zones of sub-grains and recrystallized grains (average grain size variation 35–45 μm) are located along grain boundaries and deformation band boundaries. Rare deformation lamellae appear to be sub-basal. Feldspar grains may account for up to 10% of the total rock composition and usually contain fractures. Phyllosilicates usually account for less than 10% of the total rock composition.

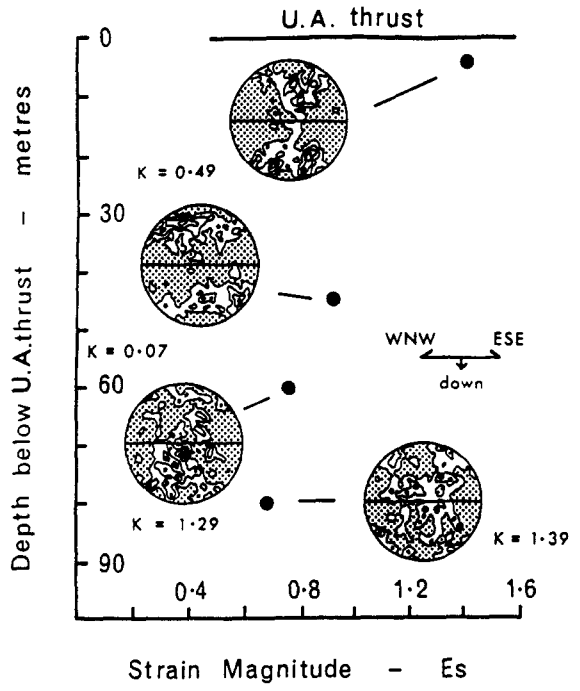

Fig. 6. Variation in calculated finite strain within the Arnaboll thrust sheet. Data taken from Dayan (1981). Es = natural logarithmic octahedral strain, k = Flinn's strain symmetry parameter. Corresponding quartz c axis fabrics (traced downwards from the Upper Arnaboll thrust) of specimens 41481, 41483, 41484 and 41482 are indicated. For explanation of contour intervals see Fig. 2.

At higher structural levels, close to the Upper Arnaboll thrust, the detrital quartz grains become more elongate and recrystallization and deformation bands are more common. A small increase in the phyllosilicate content is also detected. Ribbon-like detrital quartz grains are found in the most highly deformed specimens (Fig. 7b).

Strain-analysis results from the Arnaboll thrust sheet at Kempie are shown in Fig. 6. Note the apparent increase in strain magnitude as the Upper Arnaboll thrust is approached, and also the change in strain symmetry from almost plane strain (k = 1) at distances of 60–80 m below the Upper Arnaboll thrust to flattening strains (k = 0) closer to the thrust. It should be noted, however, that the two specimens exhibiting approximate plane strain were collected from the hinge of a major fold. Thus strain magnitude and symmetry may not bear a simple relationship to depth beneath the Upper Arnaboll thrust.

Maximum extension directions (X) calculated from these specimens trend approximately NW–SE, in a vertical plane aligned sub-parallel to the inferred WNW transport direction of the thrust belt. Using the detrital grain shape data alone, it is uncertain whether the finite oblate strains exhibited by some of these specimens indicate a real extension parallel to the strike of the thrust belt or are, for example, a reflection of a more complex deformation path, or an initial sedimentary fabric.

Quartz c axis preferred orientation patterns within the Arnaboll thrust sheet

Quartz c axis preferred orientation patterns measured in detrital grains are shown in Fig. 8. Specimens with calculated flattening strains (k = 0) display detrital c axes which lie on a small circle girdle (opening angle 25–35°) about the calculated minimum principal strain

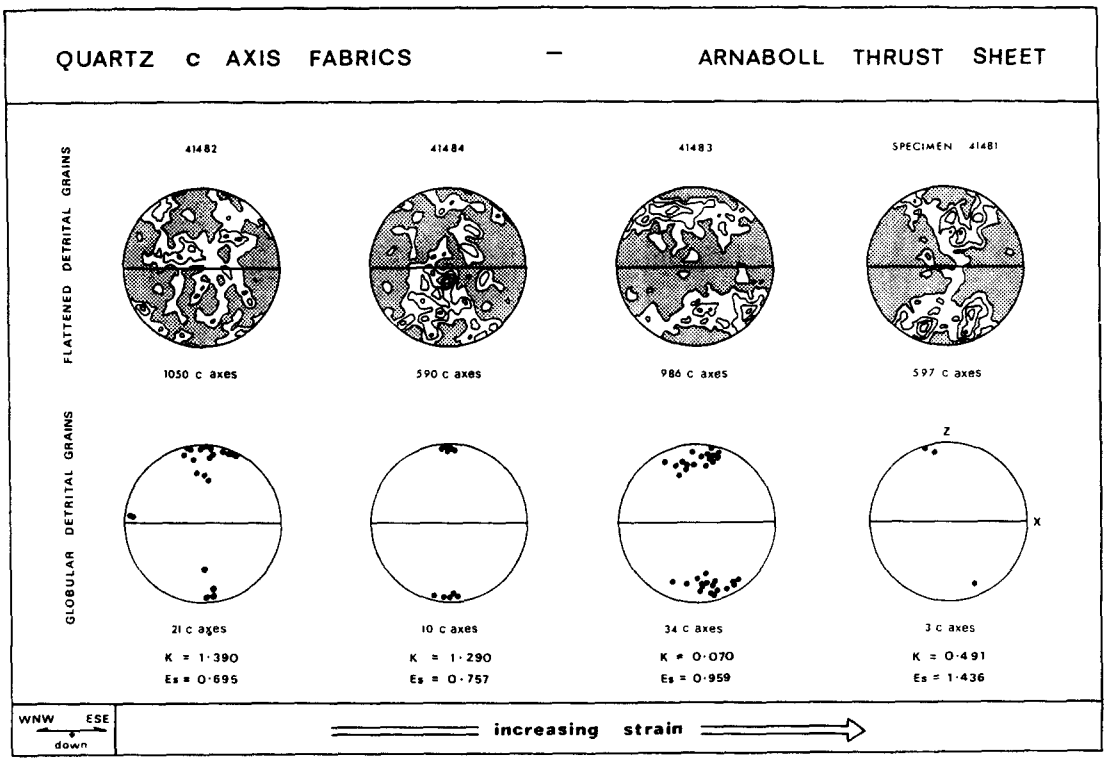

Fig. 8. Quartz c axis fabrics from the upper levels of the Arnaboll thrust sheet. XY plane of the calculated strain ellipsoid vertical, maximum extension direction (X) horizontal. Geographical orientation of stereograms indicated. For specimen location and explanation of contour interval see Fig. 2.

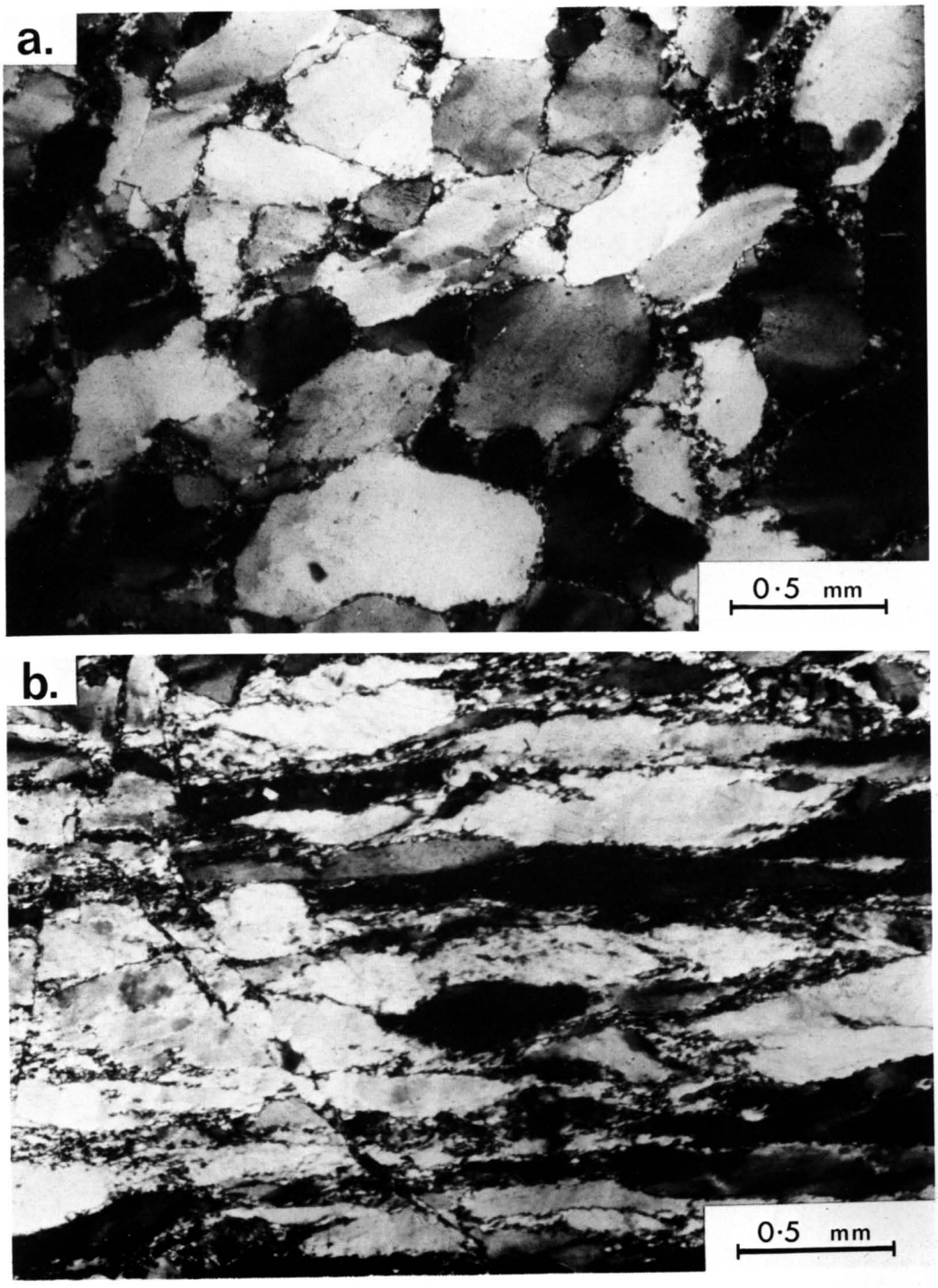

Fig. 7. Photomicrographs of quartzites collected from the upper and central levels of the Arnaboll thrust sheet. Thin sections cut perpendicular to mylonitic foliation and approximately parallel to grain shape lineation. (a) Slightly deformed quartzite. Note recrystallization at detrital quartz grain boundaries and weak deformation bands within detrital quartz grains. (b) More highly deformed quartzite. Mylonitic foliation defined by preferred alignment of elongate detrital quartz grains. Note widespread recrystallization at grain boundaries and off-set of mylonitic foliation along well-defined fractures.

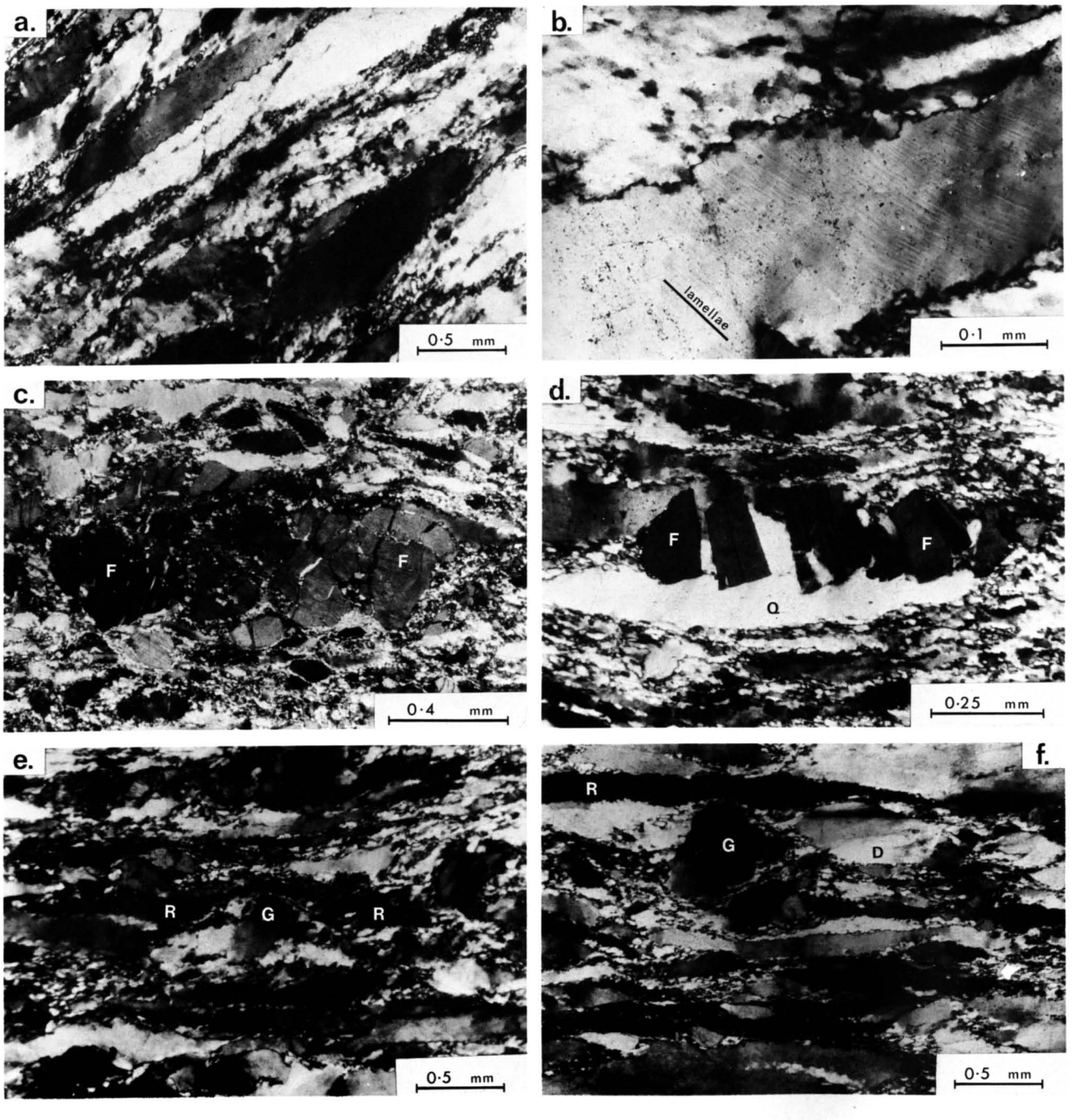

Fig. 9. Photomicrographs of quartzites collected from the upper and central levels of the Upper Arnaboll thrust sheet. Thin sections cut perpendicular to mylonitic foliation and approximately parallel to grain-elongation lineation. (a) Mylonitic foliation (trace trends top right to bottom left) defined by a preferred alignment of elongate quartz grains. (b) Lamellae (orientation indicated) within a deformed quartz grain. Universal stage work indicates that these lamellae are sub-basal in orientation. (c) Large fractured feldspar grain (F) within a matrix of smaller, plastically deformed and recrystallized, quartz grains. Note that fractures within the feldspar grain are orientated at a high angle to the mylonitic foliation (trace horizontal) defined by a preferred alignment of elongate quartz grains. (d) Fractured feldspar grain (F) within a matrix of smaller, plastically deformed and recrystallized quartz grains. Note that fractures within the feldspar grain are orientated at a high angle to the mylonitic foliation (trace horizontal) and are parallel to the feldspar twin lamellae. Considerable dilation is associated with these fractures which are infilled with quartz which is in optical continuity with the adjacent quartz grain (Q). (e) Highly elongate quartz grain (R) anastomosing around a globular quartz grain (G) whose *c* axis is aligned sub-perpendicular to the mylonitic foliation defined by elongate quartz grains. (f) Variation in morphology of deformed quartz grains. Note the presence of globular (G) and highly elongate or 'ribbon-like' (R) quartz grains together with quartz grains displaying less extreme aspect ratios (D).

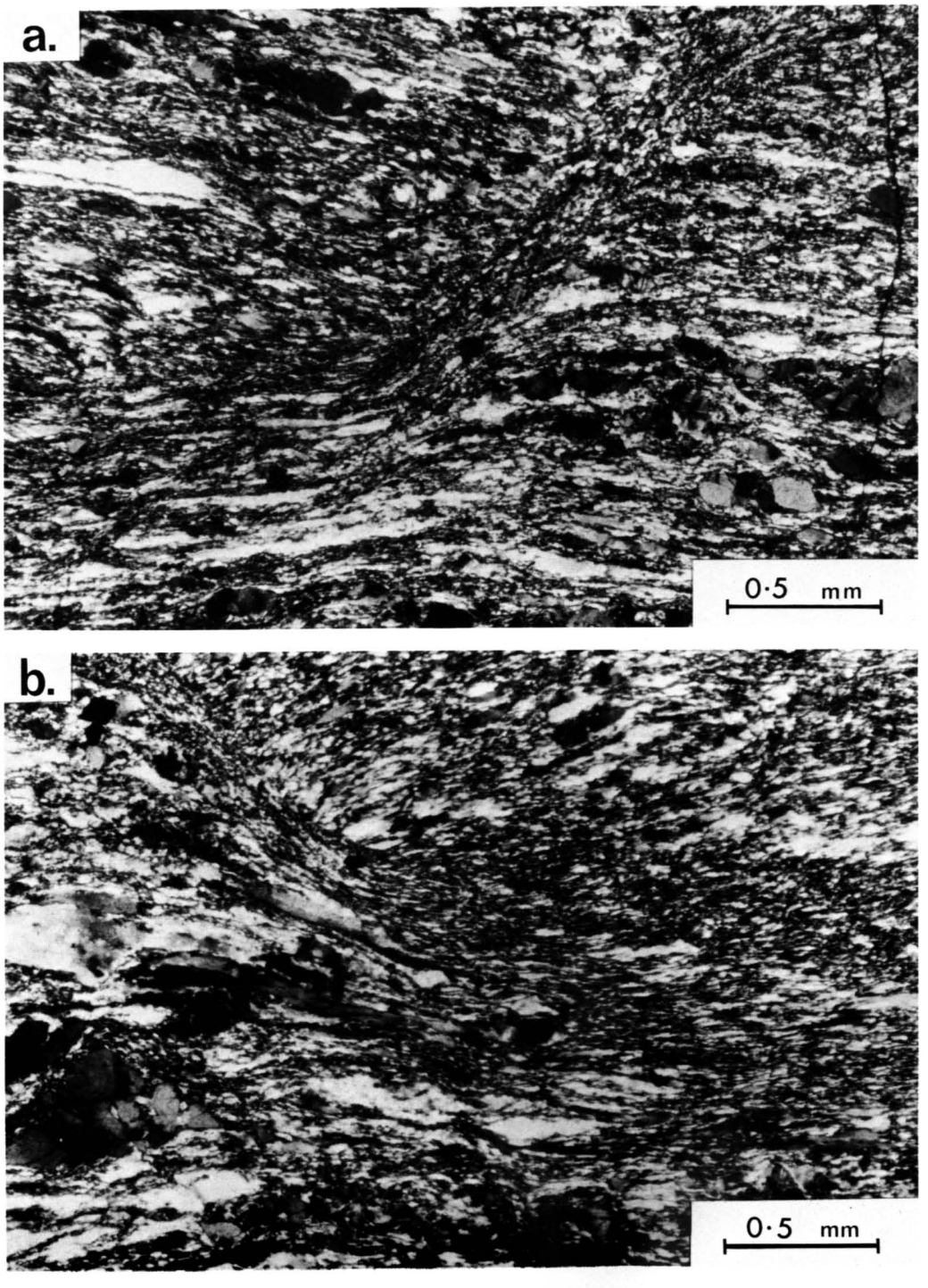

Fig. 12. Photomicrographs (viewed towards the NNE) of 'shear bands' within the central levels of the Upper Arnaboll thrust sheet. Conjugate, mutually interfering sets of these 'shear bands' which are symmetrically disposed with respect to foliation are locally observed within the upper and central levels of the Upper Arnaboll thrust sheet. Both photomicrographs (a) & (b) were taken from one thin section (orientated perpendicular to mylonitic foliation and parallel to grain shape lineation) prepared from specimen 41472. Trace of mylonitic foliation in both (a) & (b) is horizontal. 'Shear band' traces in (a) & (b) trend top right to bottom left and top left to bottom right, respectively. Note widespread recrystallization of quartz within 'shear bands'.

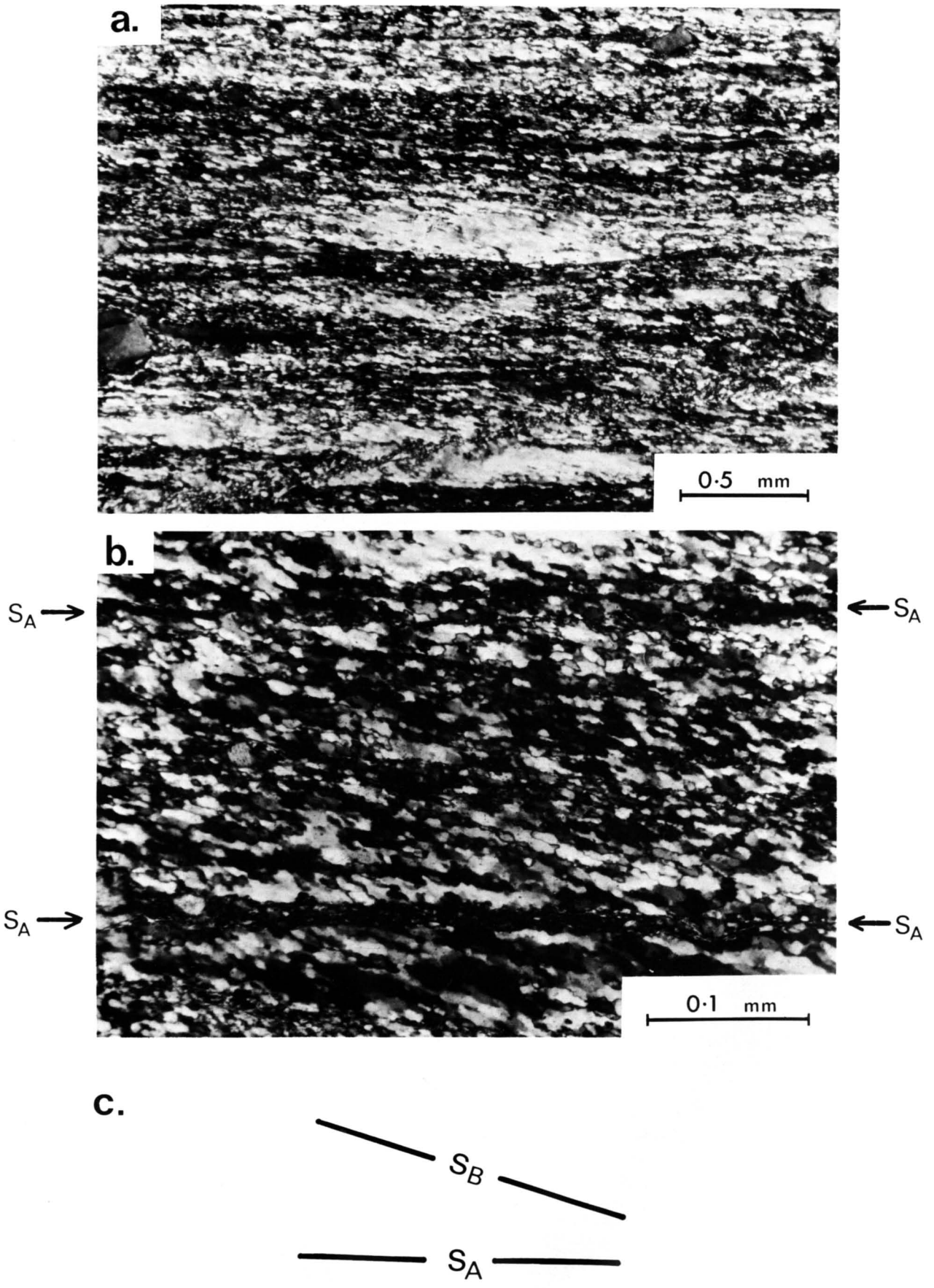

Fig. 16. Photomicrographs (viewed towards the NNE) of quartzites collected from the lower levels of the Upper Arnaboll thrust sheet. Two foliations are always observed in thin section cut perpendicular to the mylonitic foliation (S_A) and parallel to the grain shape lineation in these highly recrystallized quartzites. The most obvious foliation (a) is a spaced foliation (S_A) defined by the boundaries of 'ghost' detrital quartz grains which have suffered intense recrystallization. It is along these surfaces that the quartzites cleave in hand specimen. Between these spaced cleavage zones are located domains of recrystallized quartz grains containing a second foliation (S_B) which is oblique to S_A and defined by the preferred grain shape alignment of recrystallized quartz grains (b). Sinistral shearing is indicated by petrofabric analysis of these quartzites. (a) Mylonitic foliation (S_A) defined by a preferred alignment of highly recrystallized 'ghost' detrital quartz grains. Note a preferred alignment of elongate recrystallized quartz grains (trending top left to bottom right) defining a second foliation (S_B), which is oblique to S_A. (b) Preferred alignment of elongate recrystallized quartz grains defining S_B. Note the presence of spaced S_A foliation domains (horizontal traces located between arrows labelled S_A). (c) Relative orientation of S_A and S_B traces in (a) & (b).

direction (Z). For specimens that indicate approximate plane strain ($k = 1$) a cross girdle fabric is observed, consisting of a small circle girdle (of similar opening angle) about Z, and connected through Y.

There is some resemblance between these quartz c axis fabrics and those predicted by Lister *et al.* (1978) when basal $<a>$ glide is the easiest slip system to operate and the r and z systems have equal but higher critical activation stresses. However, the low intensity of the detected fabrics renders exact correlation difficult. The majority of these c axis fabrics are symmetrically disposed (both in terms of skeletal outline and intensity distribution) with respect to foliation and lineations. Globular detrital quartz grains, around which more flattened quartz grains may anastomose, are found to have their c axes aligned (Fig. 8) at low angles to Z. In later discussion it will be argued that these observations indicate a coaxial deformation history.

The quartz c axis fabrics indicate that the calculated apparent extensions (Dayan 1981) both parallel to the vertical plane containing the inferred thrust transport direction and parallel to the strike of the thrust belt are real extensions, and not the result of superimposed deformation phases or an initial sedimentary fabric.

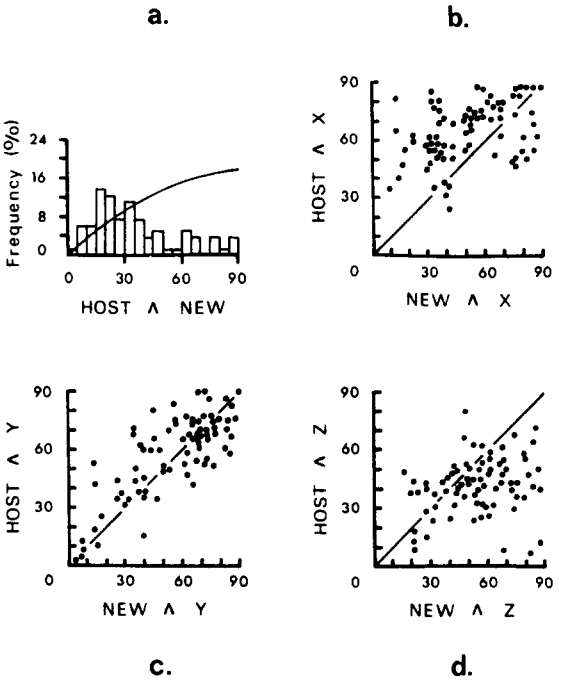

Fig. 10. Angular relationships between c axes of host (detrital) and new (recrystallized) quartz grains and principal axes of calculated strain ellipsoid. In all cases new grains are observed in thin section to be enclosed within host detrital grains. One hundred host: new grain c axis relationships measured. (a) Frequency distribution of angles between c axes of related pairs of host and new grains. Curve superimposed on histogram represents the calculated distribution of random new grain orientations (Plummer 1940). (b)–(d) Angular relationships between c axes of related pairs of host and new grains and the X, Y and Z axes of the calculated finite strain ellipsoid, respectively. Lines of equal angular relationship indicated.

FABRIC DEVELOPMENT WITHIN THE UPPER ARNABOLL THRUST SHEET

Microstructure and strain analysis of quartzites within the upper and central levels of the Upper Arnaboll thrust sheet

Detrital quartz grains within the Upper Arnaboll thrust sheet generally have a more highly flattened appearance than those within the Arnaboll thrust sheet. Within the Upper Arnaboll thrust sheet less strongly deformed quartzites are found within the upper and central levels of the thrust sheet, being particularly common to the east of Loch Hope (Fig. 2).

Detrital quartz grains from quartzites in this structural position commonly display length–width ratios of 5:1 and a well-defined preferred orientation of clast long axes in thin sections cut approximately parallel to the XZ plane (Fig. 9a). Undulatory extinction and deformation bands are more strongly developed than within quartzites of the Arnaboll thrust sheet. Deformation lamellae are observed within some of the less flattened detrital quartz grains and are typically sub-basal in orientation. These lamellae are particularly abundant in specimen 41504 (Fig. 9b).

Recrystallization is commonly observed in zones around detrital quartz grain margins and also along deformation-band boundaries. Recrystallized grain size, taking into consideration stereologic effects (Dayan 1981) varies from 60 to 35 μm. Subgrains and new grains of similar size are less commonly observed within the detrital grains in low strain specimens, but are more common in higher strain specimens. The angular relationship between host detrital grain c axes and c axes of new grains located within these grains is shown in Fig. 10(a). It should be noted that these new grains are located within the interior of the detrital host grain and are not located along structures such as deformation-band boundaries. A clear angular relationship between new and host grains is detected. This angular relationship is similar to that observed in experimentally deformed quartzites by Hobbs (1968) and naturally deformed quartzites by Ransom (1971) and Bell & Etheridge (1976). These authors attribute this relationship to a host grain control over the process of recrystallization. However, as shown in Figs. 10(b)–(d), the interpretation for the quartzites described in this paper would appear to be more complex as the final orientation of new grain c axes appears to have involved a relative rotation of the host c axis away from Z towards X, the angular relationship between host c axis and Y being very similar to that between the new grain c axis and Y. Identical relationships have been detected by Law within the Roche Maurice Quartzites of Western Brittany and are the subject of current research.

Feldspar may form up to 10% of the total rock composition. The feldspar grains are commonly twinned and fractured (Fig. 9c), the fractures usually being at a high angle to the foliation, and commonly in conjugate sets fairly symmetrically orientated relative to the foliation. These fractures sometimes appear as simple-shear fractures, whilst others appear to be dilational in nature, indicating extension parallel to the foliation and grain

shape lineation, observed in hand specimen. The dilational fractures are infilled with quartz which may appear either as a single crystal infilling the fractures (Fig. 9d), or as highly recrystallized material. As in the Arnaboll thrust sheet, phyllosilicates form less than 2% of the total rock composition.

The flattened detrital quartz grains are observed to anastomose around feldspar grains and also globular quartz grains whose *c* axes are aligned at a low angle to *Z* (Fig. 9e).

In more intensely foliated and lineated specimens, some flattened detrital quartz grains have a ribbon-like appearance, whilst others exhibit less extreme aspect ratios (Fig. 9f). Recrystallization is more prominent than in the lower strain specimens, particularly along quartz grain boundaries and deformation-band boundaries. Intense recrystallization along deformation-band boundaries results in the dividing up of the original detrital quartz grain into smaller relict grains, often with more extreme aspect ratios than that of the original detrital grain. Clearly, these relics cannot be used as strain markers. Phyllosilicates have also been observed within these deformation band boundaries; trails of these phyllosilicates may be traced out from the deformation band boundaries into the recrystallized matrix.

Within the more highly deformed quartzites the foliation defined by highly flattened detrital quartz grains is observed to be deformed by a series of spaced, asymmetric crenulations. These microstructures are thought to be analogous to the 'shear bands' of White *et al.* (1980) and the extensional crenulation cleavage of Platt and Vissers (1980). Two sets of these shear bands, with opposite senses of displacement are observed forming conjugate sets (Fig. 11), with no consistent displacement of one set by the other. The acute angle defined by the intersection of these shear bands is bisected by the specimen foliation, the shear band boundaries being commonly orientated at 30–45° to the specimen foliation. The strike of these shear bands is perpendicular to the specimen lineation. Within the shear bands the specimen foliation has been subjected to considerable shear strains (Fig. 12) and intense quartz recrystallization is locally observed within them. The recrystallized quartz grain size within the shear bands (15 μm) is much smaller than that outside the shear bands (30 μm).

Strain analysis results (Dayan 1981) from the Upper Arnaboll thrust sheet are shown in Fig. 4. All results plot within the field of apparent flattening, specimens with lower strain magnitudes exhibiting more oblate strain. With an increase in calculated strain magnitude, the quartzites become more conspicuously foliated and also develop a strong grain-shape lineation within the foliation. Due to extensive recrystallization of the detrital quartz grains, strain analysis could not be carried out on these highly deformed quartzites. All are *L–S* tectonites, in which the foliation dips gently to moderately to the SE, whilst the lineation plunges to the ESE in a vertical plane also containing the inferred thrust transport direction.

As previously described, recrystallization of detrital quartz grains is observed to become more common with increasing strain magnitude, being particularly common along grain boundaries and deformation band boundaries. Recrystallization within the relatively undistorted crystal lattice between these microstructural sites is less common and often appears to begin selectively within those detrital quartz grains whose *c* axes lie on a girdle dipping to the WNW, and which are also orientated at a high angle to *Y* (Fig. 14). A kinematic model offering an explanation for this selective recrystallization will be the subject of a separate paper.

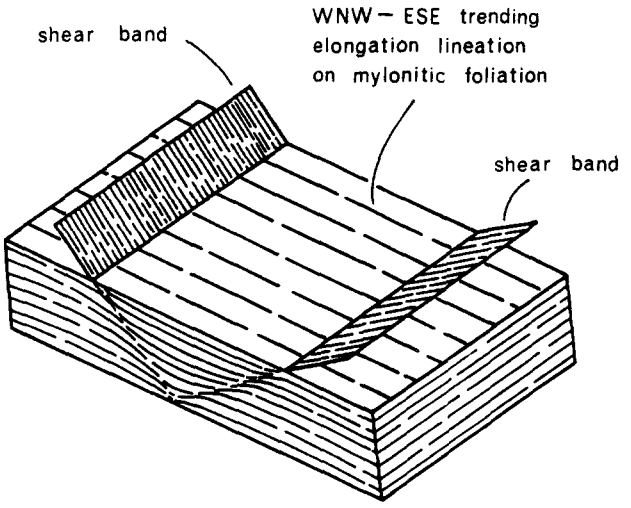

Fig. 11. Diagrammatic illustration of conjugate shear bands within the upper and central levels of the Upper Arnaboll thrust sheet.

Microstructural evidence for late brittle deformation has been observed within some of the quartzites collected from the upper and central levels of the Upper Arnaboll thrust sheet, being particularly common to the east of Loch Hope. This brittle deformation may be indicated by single fractures which off-set the mylonitic foliation (which is defined by a preferred alignment of plastically deformed detrital quartz grains) whilst in other cases the mylonitic foliation is off-set along zones (0.3–0.75 mm wide) of intensely brecciated mylonite. These zones of cataclasis divide the quartzites into a series of fault blocks. It is interesting to note that little relative rotation of the mylonitic foliation and associated quartz *c* axis fabrics has been observed between adjacent fault blocks.

Quartz c axis preferred orientation patterns within the upper and central levels of the Upper Arnaboll thrust sheet

The geographic distribution of *c* axis fabrics obtained from within the Upper Arnaboll thrust sheet is shown in Fig. 2.

Specimens, such as 41504 (Figs. 2 and 5) with calculated flattening strains display detrital quartz *c* axes which lie on a small circle girdle (opening angle 25–35°) about *Z*. For specimens that indicate approximate plane strain (Figs. 5 and 15) a cross girdle fabric is detected consisting of an elliptical girdle symmetrically disposed about *Z* (opening angle 22.5–30° in *XZ*, approximately

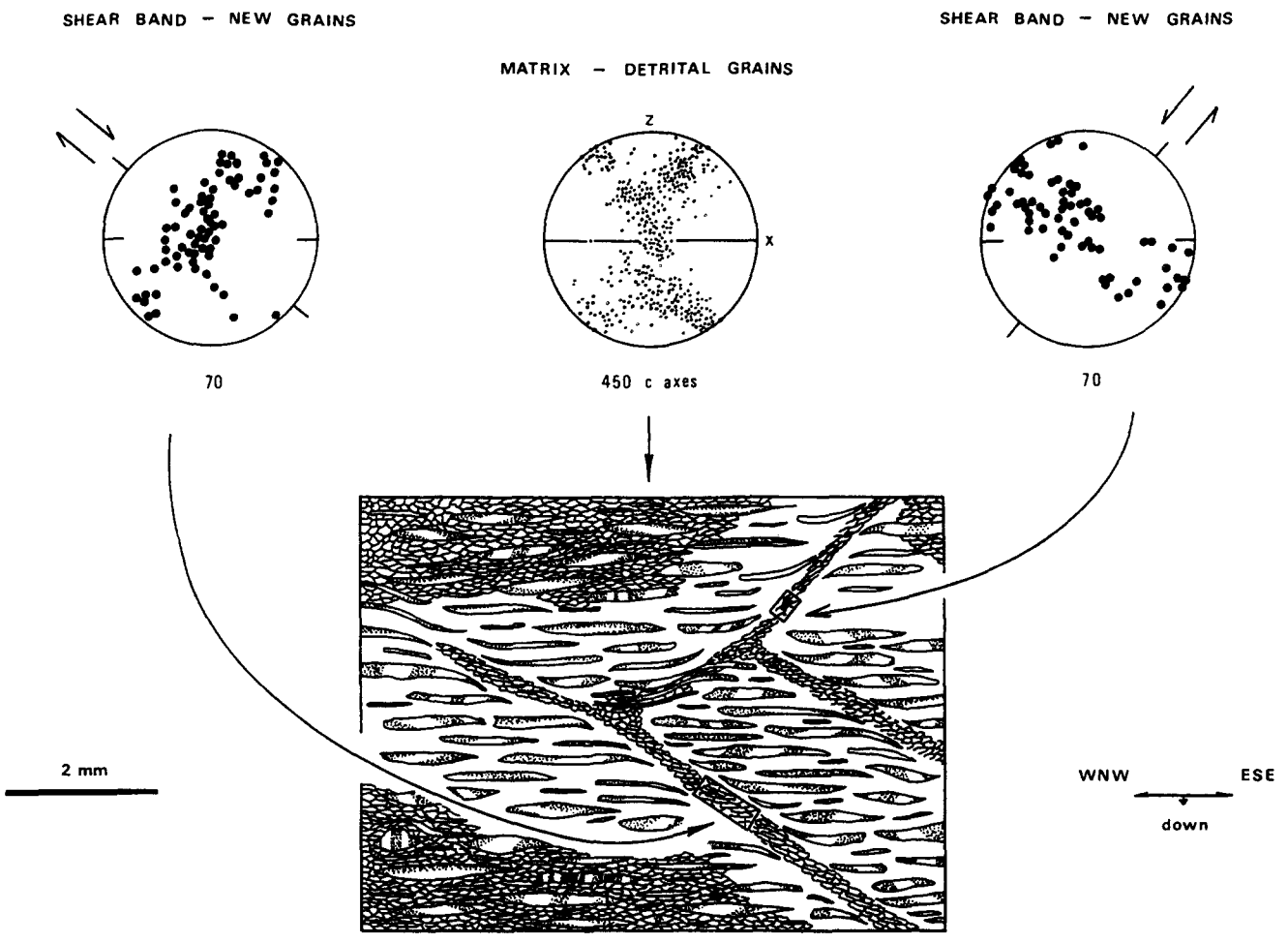

Fig. 13. Domainal quartz *c* axis fabrics associated with conjugate 'shear bands' in the upper and central levels of the Upper Arnaboll thrust sheet.

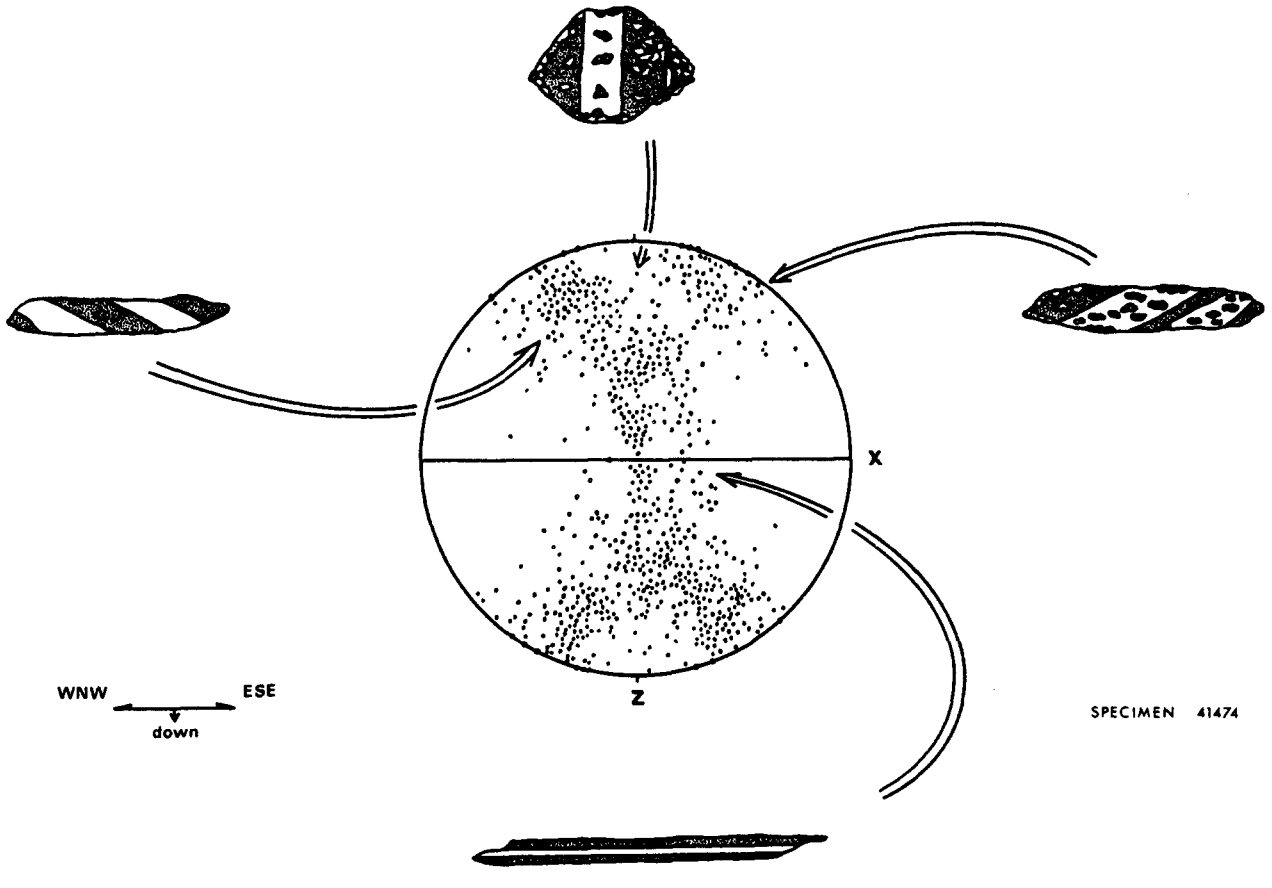

Fig. 14. Relationships between shape of deformed detrital quartz grains, the orientation of their *c* axes relative to foliation and lineation, and selective recrystallization within the central levels of the Upper Arnaboll thrust sheet. Deformation bands and selective recrystallization indicated. For specimen location see Fig. 2.

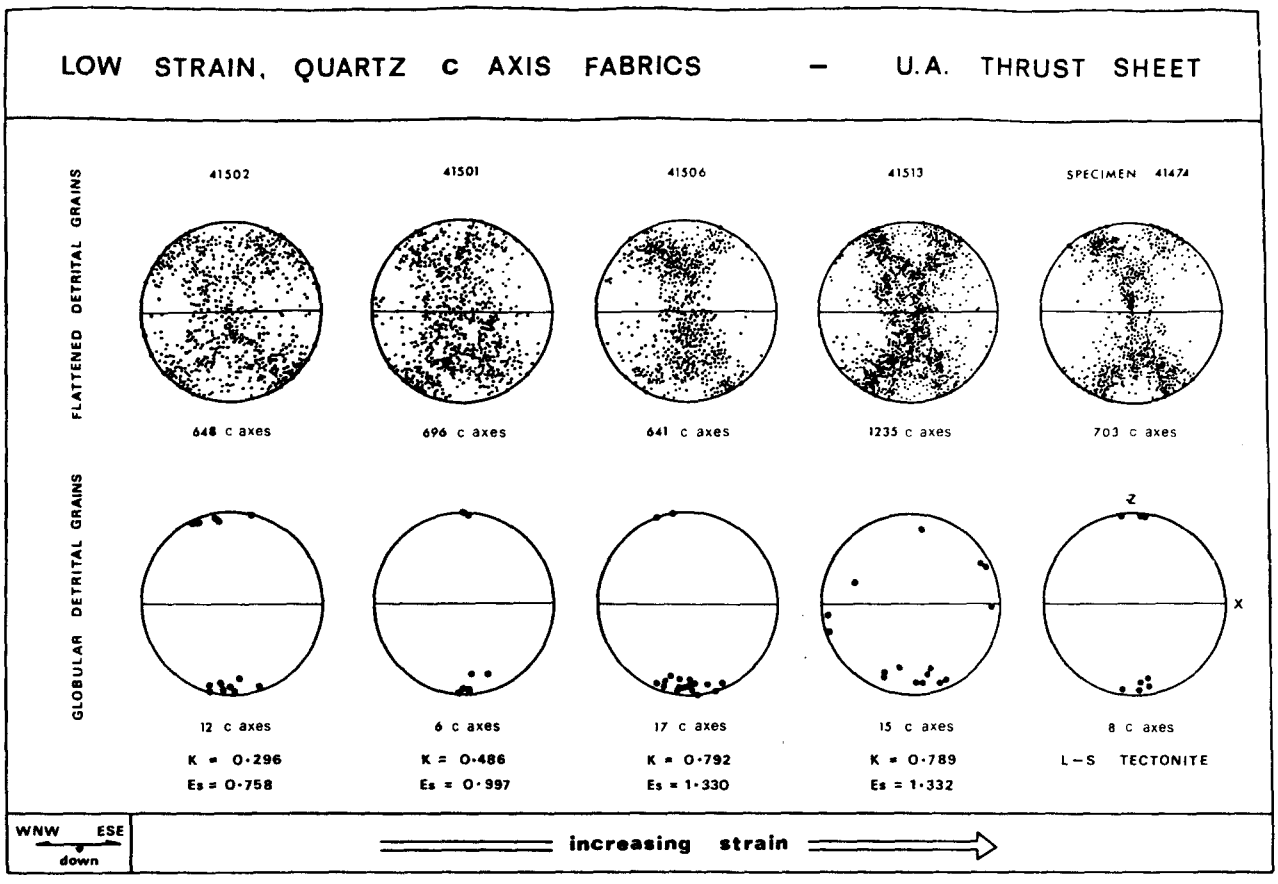

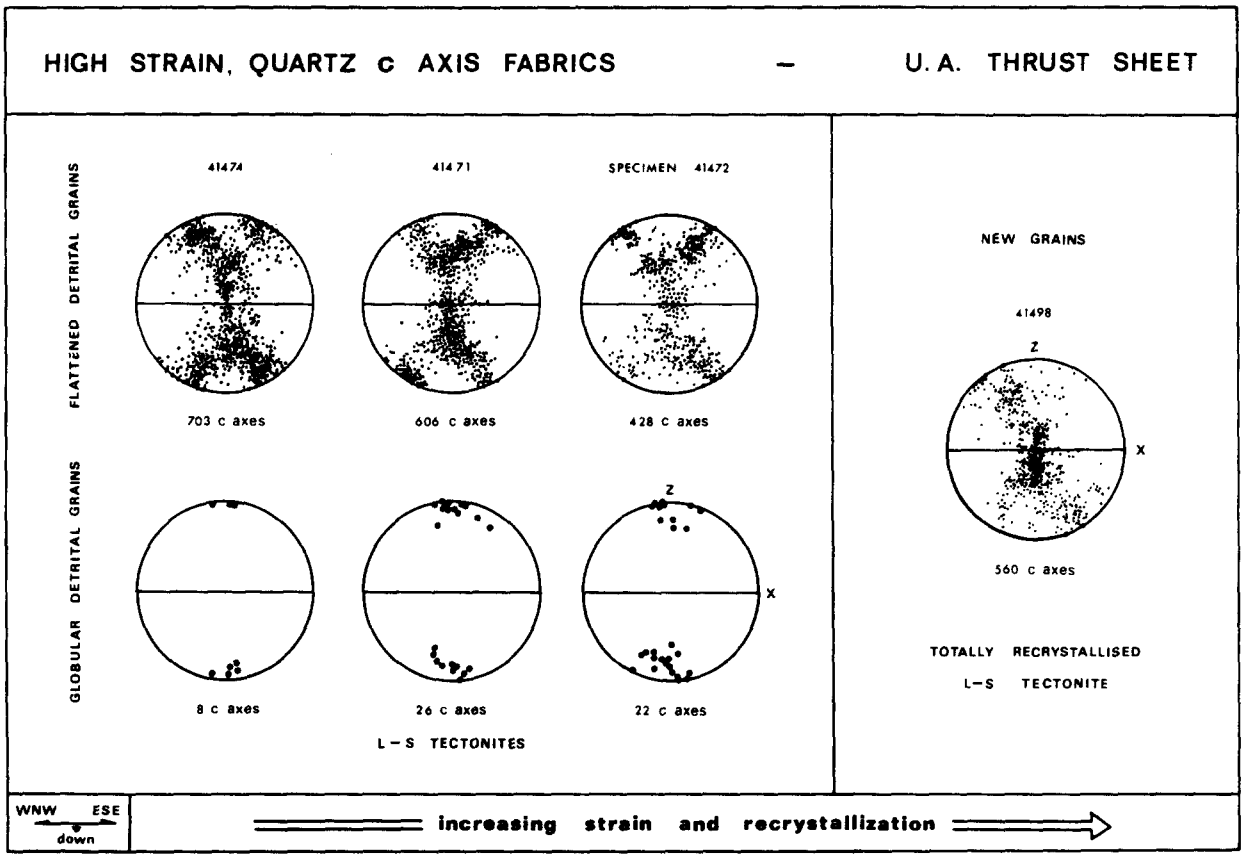

Fig. 15. Quartz *c* axis fabrics from the upper and central levels of the Upper Arnaboll thrust sheet. In specimens where strain analysis was possible, the maximum extension direction (X) is horizontal and XY plane vertical. In specimens where recrystallization was too intense for strain analysis, lineation is horizontal and foliation vertical. Location of specimens indicated in Fig. 2. Specimen 41498 is considered to have been collected from the boundary region between the central and lower levels of the thrust sheet. Geographical orientation of stereograms indicated.

40° in *YZ*) and connected through *Y*. With increasing strain (Fig. 15) these Type One (Lister 1977) cross girdle fabrics become more distinctly defined as the degree of *c* axis preferred orientation of detrital grains increases. However, the increase in strain is accompanied by progressive recrystallization of the detrital quartz-grain strain markers so that quantitative strain analysis becomes impossible. These fabrics are very similar to those predicted by Lister *et al.* (1978) when prism <*a*> glide is considerably easier to activate than glide on basal <*a*> and combined rhomb systems.

It should be noted (Fig. 15) that the *c* axis fabrics are symmetrically disposed (both in terms of skeletal outline and intensity distribution) with respect to foliation and lineation. Detrital quartz grains whose *c* axes are aligned at low angles to *Z* are observed to be globular in outline (Fig. 9e). More flattened detrital quartz grains anastomose around these globular grains. In later discussion it will be argued that these features are indicative of a coaxial deformation history.

Within these quartzites collected from the upper and central levels of the Upper Arnaboll thrust sheet, the presence of conjugate, mutually interfering shear bands (Fig. 11) symmetrically disposed with respect to the foliation is considered to be a possible third line of evidence indicating coaxial deformation (Platt & Vissers 1980). Intense recrystallization of quartz has locally taken place within these shear bands leading to the development of a strong crystallographic preferred orientation (Fig. 13). *C* axes from these shear bands define single-girdle patterns which are orientated perpendicular to the shear band boundaries. In later discussion it will be argued that the non-coaxial deformation, probably approximating to simple shear, is confined to the shear bands within these quartzites.

Microstructure of quartzites within the lower levels of the Upper Arnaboll thrust sheet

In thin section (Fig. 16a) these *L–S* tectonites are seen to have suffered intense recrystallization. The original detrital grains have undergone almost total recrystallization and are represented, in approximate *XZ* thin sections, by elongate or ribbon-like areas of new grains with similar crystallographic orientation. These 'ghost' detrital grains have their long axes aligned parallel to the specimen foliation and commonly display length–width ratios of 50:1. Two foliations are always observed in thin sections cut perpendicular to the foliation and parallel to the lineation in these highly recrystallized quartzites (Fig. 16b).

The most obvious foliation (S_A) is a spaced (0.15–0.75 mm) foliation defined by the boundaries of elongate 'ghost' detrital quartz grains referred to above. The periodicity of this foliation appears to be controlled by the width of the 'ghost' detrital grains. Phyllosilicates, commonly forming up to 5% of the total rock composition, are aligned within this spaced foliation, which anastomoses around the highly elongate 'ghost' detrital grains. In one specimen (41498) elongate new quartz grains are aligned within and parallel to the spaced foliation. This foliation (S_A) observed in thin section is parallel to the single foliation seen in hand specimen.

Between these spaced cleavage zones are located domains of recrystallized quartz grains containing a second foliation (S_B) oblique to the foliation (S_A) described above (Fig. 16b). The shape of these grains, in thin sections cut perpendicular to the single macroscopic foliation (S_A) and parallel to the lineation lying within S_A, varies from equant to highly elongate, the latter being the dominant grain type (although containing equant subgrains) with aspect ratios of up to 3:1. Typical dimensions are length and width measurements of 20–40 μm and 8–25 μm, respectively. More extreme aspect ratios are not uncommon. These elongate grains display a distinct preferred alignment of their long axes (Fig. 16). It is this preferred grain shape alignment of recrystallized quartz which imparts the second foliation (S_B) to these quartzites which is oblique to the spaced (S_A) foliation. A consistent relationship is always observed between S_A and S_B and the inferred WNW direction of overthrusting (Fig. 17); S_B always dips more steeply to the ESE than S_A. Similar microstructural relationships have been observed within shear zones by Lister & Snoke (pers. comm.) and Simpson & Schmid (1983).

A decrease in recrystallized quartz grain size within the Upper Arnaboll thrust sheet as the Upper Arnaboll thrust is approached has been noted by Dayan (1981). One specimen collected from the base of the Upper Arnaboll thrust sheet, immediately adjacent to the Upper Arnaboll thrust displays typical recrystallized quartz grain length and width measurements of 15 and 5 μm, respectively.

Within these highly recrystallized quartzites, feldspar is usually present as either large single rounded grains or as trails of much smaller rounded grains aligned parallel to S_A. Globular 'ghost' detrital quartz grains, corresponding to the similarly shaped detrital quartz grains observed in the central and upper levels of the Upper Arnaboll thrust sheet, are rarely seen.

Mutually interferring conjugate shear bands have not been observed within the highly recrystallized quartzites located within the lower levels of the Upper Arnaboll thrust sheet. Within these quartzites a single set of locally developed asymmetric crenulations deflecting S_A and S_B is observed. These crenulations strike perpendicular to the WNW–ESE trending grain shape lineation observed on S_A in hand specimen. If these crenulations are interpreted as shear bands they have geometrical properties which are consistent with the inferred WNW overthrusting of the thrust belt.

Quartz c axis preferred orientation patterns within the lower levels of the Upper Arnaboll thrust sheet

The *c* axis fabrics of new grains (Fig. 17) from highly recrystallized quartzites in the lower levels of the Upper Arnaboll thrust sheet are distinctly asymmetric with respect to the main foliation (S_A). The observed pattern of new grain quartz *c* axis preferred orientation and the

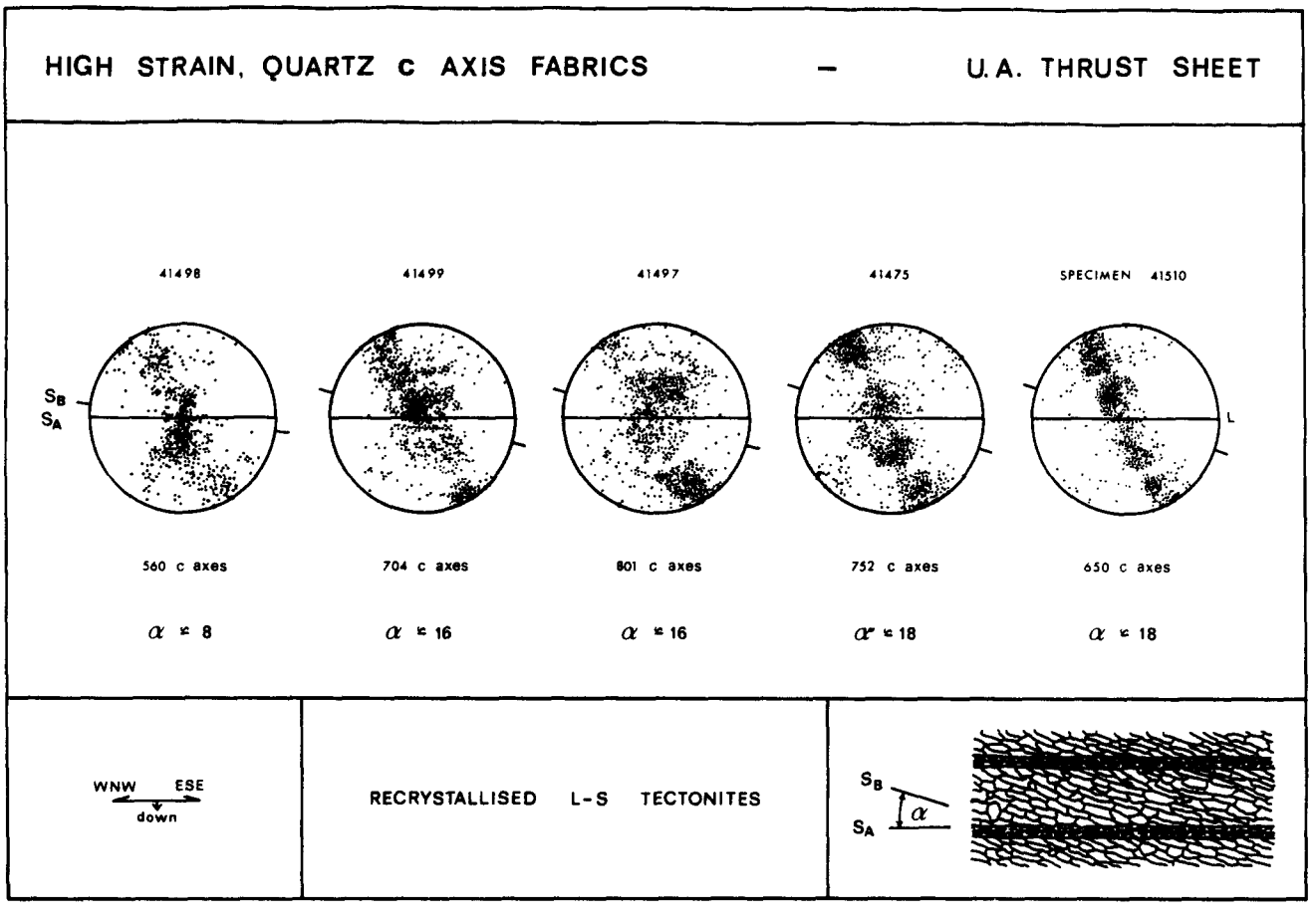

Fig. 17. Quartz *c* axis fabrics from the lower levels of the Upper Arnaboll thrust sheet. All *c* axes measured in new (recrystallized) grains. Foliations (S_A and S_B) vertical, lineation on S_A horizontal. Spatial and angular relationships between S_A and S_B together with geographical orientation of stereograms indicated. For specimen location see Fig. 2.

nature of its asymmetry with respect to S_A appears to be related to the angle (α) between S_A and S_B measured in the XZ section.

When α is small (specimen 41498) the skeletal outline of a Type One (Lister 1977) cross-girdle fabric, which is approximately symmetric with respect to S_A, is detected. This skeletal outline is identical to those defined by detrital quartz grains in the central and upper levels of the Upper Arnaboll thrust sheet. However, the density distribution of *c* axes on this cross girdle is strongly asymmetric with respect to S_A, the majority of *c* axes lying on what may be described as a 'dog-leg' shaped single girdle (Fig. 17) dipping to the ESE.

This asymmetry of *c* axis distribution is also observed (Fig. 17) in specimens exhibiting higher α values. However, in these specimens the 'dog-leg' density distribution of *c* axes is more diffuse and at still higher α values (specimen 41475) is probably better described as a planar distribution. Note that a cross girdle skeletal outline is still observed in these quartzites. In specimen 41510 very little evidence of a cross girdle fabric was detected, the vast majority of new grain quartz *c* axes defining a single girdle which dips to the ESE.

Measured in the XZ plane, a constant angular relationship between S_B and quartz *c* axis density distribution is detected, the girdle containing the majority of *c* axes being inclined at 45 (±3°) to S_B. This is in contrast with the more variable angular relationship between S_A and the quartz *c* axis density distribution.

KINEMATIC INTERPRETATION OF MICROSTRUCTURES

Two major microstructural features encountered in this study are considered to provide important information on the kinematics of deformation within the thrust sheets studied. The first important observation is the presence of globular detrital quartz grains, around which more flattened detrital quartz grains may anastomose, within the upper and central levels of the Arnaboll and Upper Arnaboll thrust sheets. These globular grains are found to have their *c* axes aligned at low angles to Z (Figs. 8 and 15) and during coaxial deformation would have extremely low resolved shear stress on their theoretically most easily activated slip planes, the basal and prism planes, throughout the deformation history. In non-coaxial deformation, the globular grain crystal lattices would rotate relative to the kinematic framework and the resolved shear stress on potential slip planes would vary during the deformation history. Similar relationships between microstructure and crystallographic orientation relative to finite strain axes have been observed in experimental coaxial deformation of

quartzites (Tullis *et al.*, 1973) and in naturally deformed quartzites considered by Bouchez (1977) and Law (1981) to have been subjected to a coaxial deformation history.

Further possible evidence for coaxial deformation within the upper and central levels of the Upper Arnaboll thrust sheet is provided by the presence of conjugate, mutually interfering shear bands (Figs. 11 and 13). Conjugate shear bands have not been found within the less intensely foliated quartzites of the Arnaboll thrust sheet.

Within the lower levels of the Upper Arnaboll thrust sheet only one set of shear bands has been observed. The angular relationship between these shear bands and the mylonitic foliation (S_A) is consistent with shearing involving non-coaxial deformation associated with WNW directed over-thrusting. It is tentatively suggested that an earlier history of coaxial deformation may be indicated within some of the highly recrystallized quartzites (specimens 41498 and 41499) collected from the lower levels of the Upper Arnaboll thrust sheet, by the presence of rare, approximately globular detrital quartz grains whose *c* axes are aligned at low angles to the pole to S_A.

Two foliations (S_A and S_B) are always observed (Fig. 17) in the *XZ* section of quartzite specimens collected from the lower levels of the Upper Arnaboll thrust sheet. As previously described, S_B is defined by a preferred grain shape alignment within domains of equant to elongate recrystallized quartz grains. These recrystallized quartz domains are separated by phyllosilicate rich domains (S_A) which are oblique to S_B. Tectonites displaying this type of microstructure are referred to as 'Type Two S-C mylonites' by Lister & Snoke (pers. comm.). Measured in the *XZ* plane, a constant angular relationship between S_B and the quartz *c* axis density distribution is detected (Fig. 16), the girdle containing the majority of *c* axes being inclined at 45 ($\pm 3°$) to S_B. This is in contrast with the more variable angular relationship between S_A and the quartz *c* axis density distribution. In later discussion it will be argued that these single *c* axis girdles indicate a predominantly simple-shear deformation and that the girdles are orientated perpendicular to the shear domain boundaries. If this interpretation is correct it may be proposed that whilst S_A has been rotated towards parallelism with the shear domain boundaries, S_B has remained at 45° to these boundaries. It is tentatively suggested that this grain shape foliation (S_B) which appears to maintain a constant angular relationship to the inferred shear domain boundaries with increasing shear strain may be a steady-state foliation (Means 1981, fig. 7), preservation of the foliation with progressive deformation being achieved by cyclic dynamic recrystallization and deformation of quartz.

Variation in recrystallized quartz grain size, taking into account stereologic effects, has been studied by Dayan (1981) within the Upper Arnaboll thrust sheet and used to estimate deviatoric stresses associated with deformation. This study indicates a smaller recrystallized grain size (and therefore a higher deviatoric stress) within the lower levels of the thrust sheet compared with higher levels. Within the lower levels of the thrust sheet an average grain size, using specimens indicated in Fig. 17, of 27.15 μm (geometric means) was calculated, corresponding to deviatoric stress estimates of 67.71 MPa using the data of Twiss (1977) and 48.87 MPa using the data of Mercier *et al.* (1977). By way of contrast, within the upper and central levels of the thrust sheet an average grain size, using specimens indicated in Fig. 15, of 45.62 μm (geometric means) was calculated, corresponding to deviatoric stress estimates of 52.4 MPa using the data of Twiss (1977) and 36.13 MPa using the data of Mercier *et al* (1977). Thus, different deviatoric stress magnitudes are associated with the two kinematic domains recognized within the Upper Arnaboll thrust sheet, the higher deviatoric stress magnitudes being associated with the domain of non-coaxial deformation located near the base of the thrust sheet. In general, smaller recrystallized grain sizes were observed by Dayan (1981) in the southern sampling site near Kempie Bay than in the more northerly sampling area (Fig. 2) to the east of Loch Hope.

KINEMATIC INTERPRETATION OF QUARTZ *C* AXIS FABRICS

Within the upper and central levels of the Arnaboll and Upper Arnaboll thrust sheets, *c* axis fabrics (Figs. 8 and 15) measured in detrital quartz grains are symmetrically disposed (both in terms of skeletal outline and intensity distribution) with respect to mylonitic foliation and lineation. Several possible kinematic interpretations of this observation may be advanced.

(1) By analogy with the computer simulations of Lister *et al.* (1978) the symmetric relationships between *c* axis fabrics and mylonitic foliation and lineation may be taken to indicate a coaxial deformation history. This interpretation is in accord with the previously proposed kinematic interpretation of microstructures within these quartzites.

(2) Kinematic domains of less than thin-section scale as described by Garcia Celma (1982) may be present within these quartzites. If opposite senses of shear are dominant in adjacent domains, it is possible that indiscriminate *c* axis measurement across these domains will have an averaging effect which produces an apparent symmetric fabric. During study of the Eriboll quartzites care was taken to avoid this potential source of error.

(3) It may be argued that at very high shear strains within a zone of simple shear, foliation (S_A) will be rotated into alignment with the shear zone walls. If a stable single girdle of *c* axes orientated perpendicular to the shear zone walls is associated with this deformation, a symmetric relationship between foliation and *c* axis would be produced at very high shear strains, giving a totally false indication of coaxial deformation. However, it is emphasised that within the Eriboll study area evidence for coaxial deformation is only found within speci-

mens exhibiting relatively low finite strain magnitudes, non-coaxial deformation being indicated within the more highly deformed quartzites.

(4) It may also be argued that the observed symmetric relationship between *c* axis fabrics and foliation and lineation is due to a late coaxial overprint on an earlier fabric produced during non-coaxial deformation. For example within the Assynt region of the Moine Thrust zone (Fig. 1) quartz *c* axis fabrics which are symmetric with respect to mylonitic foliation have been interpreted by Christie (1963) as indicating a late coaxial flattening superimposed upon originally asymmetric fabrics produced by shearing deformation. Computer modelling of this situation by Lister & Williams (1979) predicts that although the final fabric will be symmetric with respect to skeletal outline, it will be asymmetric with respect to density distribution. No convincing asymmetry of density distribution has been observed in fabrics from the upper and central levels of either the Arnaboll or Upper Arnaboll thrust sheets. Further, this interpretation involving late coaxial overprint requires that symmetric fabrics will be observed within the most highly deformed quartzites. Once again it is emphasized that within the Eriboll study area evidence for coaxial deformation is only found within specimens exhibiting relatively low finite strain magnitudes, non-coaxial deformation being indicated within the more highly deformed quartzites.

Thus of the four interpretations of symmetric fabrics within the upper and central levels of the Arnaboll and Upper Arnaboll thrust sheets discussed above, the first interpretation involving a simple coaxial deformation history is preferred.

Within the lower, intensely recrystallized levels of the Upper Arnaboll thrust sheet, quartz *c* axis fabrics from recrystallized tectonites are asymmetric (Fig. 17) with respect to the mylonitic foliation (S_A) and lineation; the sense of asymmetry (Bouchez & Pecher 1976, Lister & Williams 1979, Behrmann & Platt 1982) is consistent with shearing involving non-coaxial deformation and associated WNW directed overthrusting. This interpretation is in accord with the observed angular relationship between mylonitic foliation and the single set of shear bands observed in these quartzites. With increasing intensity of foliation development, a progression is observed (Fig. 17) from fabrics which are symmetric in terms of skeletal outline with respect to foliation but asymmetric with respect to density distribution, to fabrics which are asymmetric with respect to foliation both in terms of density distribution and skeletal outline. The asymmetry of *c* axis density distribution in these fabrics is considered to be in part due to the removal of selected orientations during recrystallization. The details of this process are the subject of a separate paper. It is tentatively suggested that the apparent *c* axis fabric variation with foliation intensity may indicate a progressive overprinting of coaxial by non-coaxial fabrics due to the relative movement of material across a strain path domain boundary. At high finite strains all traces of the earlier fabric have been removed.

X-ray texture goniometry on quartzites from the Upper Arnaboll thrust sheet has recently commenced at E.T.H., Zurich, in collaboration with M. Casey and S. Schmid; preliminary results are consistent with *c* axis data obtained by universal stage methods. Deformed quartzites from the upper and central levels of the thrust sheet are characterized by two *a* axis maxima aligned within the *XZ* plane, symmetrically inclined at 25–35° to the lineation, and accompanied by geometrically necessary *a* axis sub-maxima. In contrast, quartzites from the lower levels of the thrust sheet yield a single *a* axis maxima orientated within the *XZ* plane, inclined at 25–30° to the lineation, and accompanied by geometrically necessary *a* axis sub-maxima; this single *a* axis maxima occupies the pole position to the corresponding *c* axis single girdle distribution obtained by universal stage work. The results of this texture goniometry will be the subject of a separate paper.

TECTONIC MODELS

Two kinematic domains may be recognized within the Upper Arnaboll thrust sheet; a structurally higher domain with relatively low finite strains which appears to be dominated by coaxial deformation and a lower domain with relatively high finite strains which appears to be dominated by non-coaxial deformation. No convincing difference in trend of lineations has been observed within quartzites from these two domains and intermediate principal axes of the finite strain ellipsoid (*Y*) inferred from the *c* axis density distributions and skeletal outlines are coincident. It is suggested that these domains were produced simultaneously; that is, coaxial deformation (approximately pure shear) in the upper levels was accompanied by non-coaxial deformation (involving a component of simple shear) towards the base of the thrust sheet. In this interpretation the contemporaneous maximum extension in a vertical plane parallel to the inferred WNW transport direction within both domains is emphasized. Note, however, that this interpretation does not exclude the possibility that the lower domain of non-coaxial deformation may have been active for longer. The contemporaneous partitioning of the Upper Arnaboll thrust sheet into kinematic (strain path) domains is considered to be a natural example of deformation partitioning within a flowing rock mass. This general rheological concept has previously been proposed on largely theoretical grounds by Lister & Williams (1983). A similar model involving strain path (vorticity) partitioning has been proposed for certain thrust sheets within the Betic Cordilleras of Spain by Behrmann (1982) on the basis of quartz *c* axis fabric variation. Other geological examples of strain path partitioning may include some of the Caledonide nappes of Scandinavia (Ramberg 1981, p. 135) and possibly also the Barnes Ice Cap of Baffin Island, Canada, which has been studied by Hudleston (1983).

Some *c* axis fabrics within the highly recrystallized tectonites located near the base of the Upper Arnaboll

thrust sheet are thought to indicate that non-coaxial strains have been superimposed on rocks already containing fabrics developed during coaxial deformation. This overprinting of coaxial deformation by non-coaxial deformation may be associated with two separate mechanisms. The first mechanism involves thinning of the thrust sheet (as indicated by strain analysis) and the associated migration of material towards the base of the thrust sheet. If the domain of non-coaxial deformation located at the base of the thrust sheet maintained a constant thickness then, during deformation, material from the upper coaxial domain may be carried into the domain of non-coaxial deformation. The second, alternative mechanism to account for this inferred change in deformation path would be the upward expansion with time of the lower domain of non-coaxial deformation into the domain of coaxial deformation.

The kinematic interpretation of quartz *c* axis fabrics and microstructural features involving coaxial deformation within the upper and central levels of the Arnaboll and Upper Arnaboll thrust sheets has interesting implications for strain history models within thrust sheets. Similar studies in other thrust zones such as the Himalayan Main Central Thrust (Bouchez & Pecher 1976), the Caledonian nappes of northern Norway (Boullier & Quenardel 1981), the Betic Cordilleras of Spain (Behrmann & Platt 1982) and the Moine Nappe (White *et al.* 1982) lying immediately above the Upper Arnaboll thrust sheet at Eriboll, have all revealed fabrics indicating non-coaxial, simple shear deformation. How then is it possible for coaxial deformation to take place within a thrust zone environment? Three models which can account for the observed distribution and nature of deformation are proposed below (see Figs. 18 and 19).

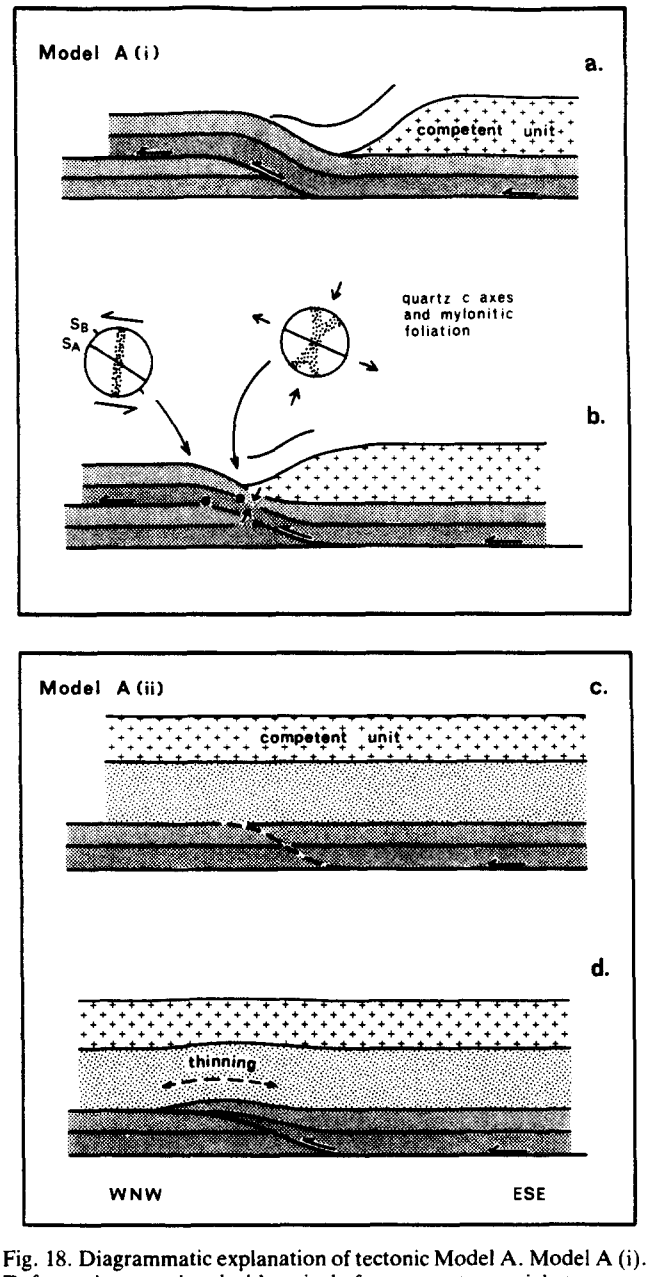

Fig. 18. Diagrammatic explanation of tectonic Model A. Model A (i). Deformation associated with arrival of competent material at a ramp. The structural locations of quartz *c* axis fabrics which may be associated with deformation of relatively incompetent quartzites lying between ramp and competent unit are indicated by large black dots. Model A (ii). Deformation associated with ramp development beneath an already emplaced thrust sheet of competent material. See text for details.

Model A

The nature and distribution of deformation recorded in the Upper Arnaboll thrust sheet may have developed in response to an active thrust attempting to carry higher level, more competent, thrust sheets over ramps. Two examples of how this situation may arise are shown in Fig. 18. For the Eriboll area the higher, more competent thrust sheets would be those containing Lewisian basement and Moine rocks.

The first example involves the arrival of the competent material at a ramp (Fig. 18a). The resistance of the competent unit to the bending needed to allow continued movement on the active fault may be relieved by thinning in the lower, weaker, thrust sheet (in this case the Cambrian quartzite). A diagrammatic illustration of the quartz *c* axis fabrics and foliation that could be associated with this deformation of the quartzites is presented in Fig. 18(b). In detail, deformation of the relatively weak Cambrian quartzites may involve shearing along discontinuities such as bedding, accompanied by coaxial thinning and extension of the quartzites between the discontinuities. This situation would be similar to the mechanism of sliding on discontinuities proposed by Lister & Williams (1979) to account for coaxial deformation in shear zones.

An alternative, though similar, necessity for thinning the thrust sheet may arise where a ramp develops under an already emplaced thrust sheet of competent material (Fig. 18c). In this situation an alternative to folding the overlying competent sheet to allow continued displacement on the active thrust plane would be to thin the weaker, lower level, thrust sheet (Fig. 18d).

A more detailed discussion of the deformation processes associated with displacement over ramps is given by Knipe (in press).

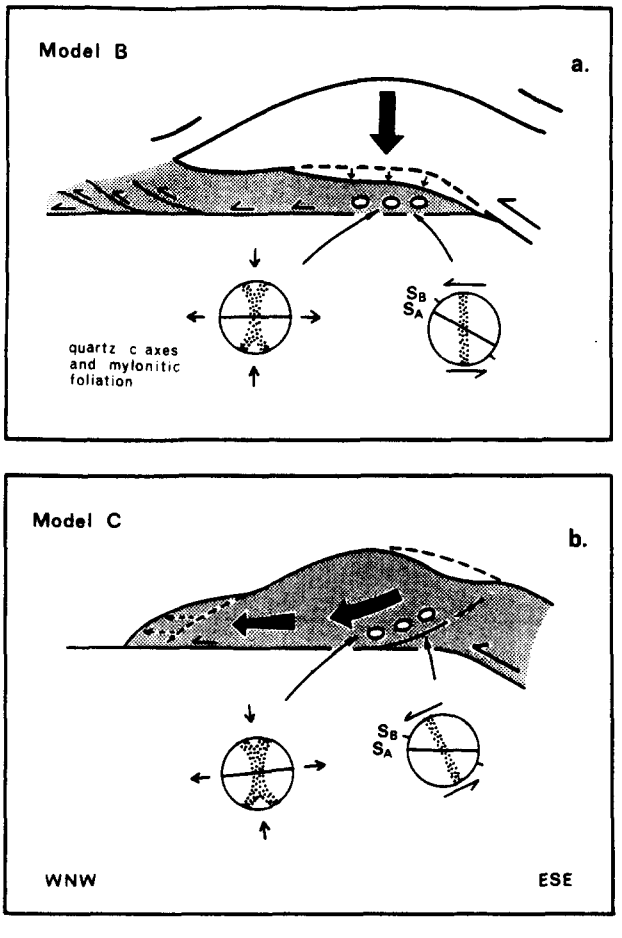

Fig. 19. Diagrammatic explanation of tectonic Models B and C. (a) Model B. Deformation associated with emplacement of a frontal culmination. Quartz *c* axis fabrics and strain ellipses which may be associated with this deformation indicated. See text for details. (b) Model C. Deformation associated with extensional flow produced by gravity spreading. Quartz *c* axis fabrics and strain ellipses which may be associated with this deformation indicated. See text for details.

Model B

In this model the domains of coaxial and underlying non-coaxial deformation are associated (Fig. 19a) with the emplacement of a frontal culmination (see Butler 1982b for terminology). Loading of material beneath the culmination may generate coaxial thinning of the lower level, less competent, thrust sheet and simultaneous extrusion accompanied by shearing. Traced towards the foreland these zones of localized shearing may have developed into a series of imbricate reverse faults (Fig. 19a).

A diagrammatic illustration of the quartz *c* axis fabrics and foliations that could be associated with the tectonic situation proposed in Model B is presented in Fig. 19(a).

Model C

In Model C (Fig. 19b) it is proposed that extensional flow (plane strain with maximum extension parallel to the transport direction) involving coaxial deformation was produced by gravity spreading (Elliott 1976) from a thickened Caledonian mass to the east. This coaxial deformation was accompanied by shearing (non-coaxial deformation) along the base of the extensional flow regime. Gravitational spreading has been postulated along the Moine Thrust zone by Coward (1982, 1983).

With the evidence available it is not possible to decide which of the three models is most applicable to the area studied.

CONCLUSIONS

The integration of field mapping, microstructural observations, strain analysis and petrofabric studies within the Eriboll area of the Moine Thrust zone leads to the following conclusions.

(1) Coaxial deformation within the upper levels of the Arnaboll thrust sheet is indicated by both microstructural and petrofabric studies.

(2) Coaxial deformation is also indicated by both microstructural and petrofabric studies within the upper and central levels of the adjacent, but structurally higher, Upper Arnaboll thrust sheet. Strain analysis suggests that this deformation involved thinning of the thrust sheet accompanied by maximum extension in the inferred thrust transport direction.

(3) The intensity of quartz *c* axis preferred orientation is directly proportional to calculated strain magnitude. A correlation is also established between pattern of *c* axis preferred orientation and the calculated strain symmetry.

(4) The most intensely deformed rocks encountered in this study are located within the lower levels of the Upper Arnaboll thrust sheet. They are all recrystallized *L–S* tectonities which exhibit asymmetrical quartz *c* axis fabrics, the sense of asymmetry being consistent with shearing involving non-coaxial deformation and associated WNW directed overthrusting.

(5) Two foliations are observed within specimens collected from the lower levels of the Upper Arnaboll thrust sheet. The most obvious foliation, defined by alternating quartz and phyllosillicate domains is correlated with the single foliation observed in the higher levels of the thrust sheet. A second folition, defined by a preferred grain shape alignment of recrystallized quartz is oblique to the domainal foliation. It is tentatively suggested that this second foliation may be a steady-state foliation.

(6) A kinematic interpretation of microstructures and quartz *c* axis fabrics from the Upper Arnaboll thrust sheet is proposed. This interpretation involves coaxial thinning and concomitant extension in a vertical plane parallel to the thrust transport direction accompanied by synchronous, similarly orientated, shearing within the lower levels of the thrust sheet.

(7) Three tectonic models are presented to explain the distribution of deformation domains. One of these models involves local thinning of a thrust sheet where more competent overlying thrust sheets resisted deformation associated with movement over a ramp. The other two models involve important gravitational components.

Acknowledgements—The authors have benefited from discussion with M. P. Coward, G. S. Lister, S. Schmid, M. Casey, R. W. H. Butler, S. H. White, D. Evans, D. H. Mainprice and G. P. Price. H. Dayan particularly wishes to thank M. P. Coward for supervising his thesis work in the Eriboll region. The work was partially supported by Natural Environment Research Council grant GR3/4612. H. Dayan gratefully acknowledges the receipt of research scholarships from the British Council and the Consecho Nacional de Desenvolvimento Technologico e Cientifico whilst at the University of Leeds. Stereograms were contoured by M. Casey at ETH, Zurich.

REFERENCES

Allison, I. 1979. Variations of strain and microstructure in folded Pipe Rock in the Moine thrust zone of Loch Eriboll and their bearing on the deformational history. *Scott. J. Geol.* **15**, 263–269.

Behrmann, J. H. 1982. Structures and deformational processes in a zone of contact strain beneath a nappe, Sierra Alhamilla, Spain. Unpublished D. Phil. thesis, University of Oxford.

Behrmann, J. H. & Platt, J. P. 1982. Sense of nappe emplacement from quartz *c* axis fabrics: an example from the Betic Cordilleras (Spain). *Earth Planet. Sci. Lett.* **59**, 208–215.

Bell, T. H. & Etheridge, M. A. 1976. The deformation and recrystallisation of quartz in a mylonite zone, central Australia. *Tectonophysics* **32**, 235–267.

Bouchez, J.-L. 1977. Plastic deformation of quartzites at low temperature in an area of natural strain gradient (Angers, France). *Tectonophysics* **39**, 25–50.

Bouchez, J.-L. & Pecher, A. 1976. Plasticité du quartz et sens cisaillement dans des quartzites du Grand chevauchement Central Himalayan. *Bull. Soc. geol. Fr.* **18**, 1377–1385.

Boullier, A. M. & Quenardel, J.-M. 1981. The Caledonides of northern Norway: relation between preferred orientation of quartz lattice strain and translation of the nappes. In: *Thrust and Nappe Tectonics* (edited by McClay, K. & Price, N. J.). *Spec. Publs geol. Soc. Lond.* **9**, 185–195.

Butler, R. W. H. 1982a. A structural analysis of the Moine Thrust Zone between Loch Eriboll and Foinaven, N.W. Scotland. *J. Struct. Geol.* **4**, 19–30.

Butler, R. W. H. 1982b. The terminology of structures in thrust belts. *J. Struct. Geol.* **4**, 239–246.

Christie, J. M. 1963. The Moine Thrust Zone in the Assynt region, northwest Scotland. *Univ. California Publ. geol. Sci.* **40**, 345–440.

Compton, R. R. 1980. Fabrics and strain in quartzites of a metamorphic core complex, Raft River Mountains, Utah. *Mem. geol. Soc. Am.* **153**, 385–398.

Coward, M. P. 1980. The Caledonian thrust and shear zones of N.W. Scotland. *J. Struct. Geol.* **2**, 11–17.

Coward, M. P. 1982. Surge zones in the Moine thrust zone of N.W. Scotland. *J. Struct. Geol.* **4**, 247–256.

Coward, M. P. 1983. The thrust and shear zones of the Moine thrust zone and the N.W. Scottish Caledonides. *J. geol. Soc. Lond.* **140**, 795–811.

Dahlstrom, C. D. A. 1970. Structural geology in the eastern margin of the Canadian Rocky Mountains. *Bull. Can. Petrol. Geol.* **18**, 332–400.

Dayan, H. 1981. Deformation studies of the folded mylonites of the Moine Thrust, Eriboll District, Northwest Scotland. Unpublished Ph.D. thesis, University of Leeds.

Dunnet, D. 1969. A technique of finite strain analysis using elliptical particles. *Tectonophysics* **7**, 117–136.

Elliott, D. 1976. The energy balance and deformation mechanisms of thrust sheets. *Phil. Trans. R. Soc.* **A283**, 289–312.

Elliott, D. & Johnson, M. R. W. 1980. The structural evolution of the northern part of the Moine thrust zone. *Trans. R. Soc. Edinb., Earth Sci.* **71**, 69–96.

Garci Celma, A. 1982. Domainal and fabric heterogeneities in the Cap de Creus quartz mylonites. *J. Struct. Geol.* **4**, 443–456.

Hobbs, B. E. 1968. Recrystallisation of single crystals of quartz. *Tectonophysics* **6**, 353–401.

Hudleston, P. J. 1983. Strain patterns in an ice cap and implications for strain variations in shear zones. *J. Struct. Geol.* **5**, 455–464.

Knipe, R. J. (in press). Footwall geometry and the rheology of thrust sheets. *J. Struct. Geol.*

Law, R. D. 1981. Relationships between strain and quartz optic axis fabrics in the Roche Maurice Quartzites of Western Brittany (abstract). *J. Struct. Geol.* **3**, 189.

Lister, G. S. 1977. Crossed-girdle *c* axis fabrics in quartzites plastically deformed by plane strain and progressive simple shear. *Tectonophysics* **39**, 51–54.

Lister, G. S., Paterson, M. S. & Hobbs, B. E. 1978. The simulation of fabric development in plastic deformation and its application to quartzites: the model. *Tectonophysics* **45**, 107–158.

Lister, G. S. & Williams, P. F. 1979. Fabric development in shear zones, theoretical controls and observed phenomena. *J. Struct. Geol.* **1**, 283–297.

Lister, G. S. & Williams, P. F. 1983. The partitioning of deformation in flowing rock masses. *Tectonophysics* **92**, 1–33.

McClay, K. R. & Coward, M. P. 1981. The Moine Thrust Zone: an overview. In: *Thrust and Nappe Tectonics* (edited by McClay, K. & Price, N. J.). *Spec. Publs. geol. Soc. Lond.* **9**, 241–260.

Means, W. D. 1981. The concept of steady-state foliation. *Tectonophysics* **78**, 179–199.

Mercier, J. C. C., Anderson, D. A. & Carter, N. L. 1977. Stress in the lithosphere: inferences from steady state flow of rocks. *Pure appl. Geophys.* **115**, 199–226.

Peach, B. N., Horne, J., Gunn, W., Clough, C. T. & Hinxman, L. W. 1907. The geological structure of the northwest Highlands of Scotland. *Mem. geol. Surv. G.B.*

Peach, C. J. & Lisle, R. J. 1979. A FORTRAN IV program for the analysis of tectonic strain using deformed elliptical markers. *Comput. Geosc.* **5**, 325–334.

Platt, J. P. & Vissers, R. L. M. 1980. Extensional structures in anisotropic rocks. *J. Struct. Geol.* **2**, 397–410.

Plummer, H. C. 1940. *Probability and Frequency*. Macmillan, London.

Ramberg, H. 1981. The role of gravity in orogenic belts. In: *Thrust and Nappe Tectonics* (edited by McClay, K. & Price, N. J.). *Spec. Publs. geol. Soc. Lond.* **9**, 125–140.

Ransom, D. M. 1971. Host control of recrystallised quartz grains. *Mineral. Mag.* **38**, 83–88.

Rathbone, P., Coward, M. P. & Harris, A. 1983. Cover and basement: a contrast in style and fabrics. In: *Tectonics and Geophysics of Mountain Chains* (edited by Harris, L. D. & Williams, H.). *Mem. geol. Soc. Am.* **158**, 213–223.

Schmid, S. M. 1975. The Glarus Overthrust: field evidence and mechanical model. *Eclog. geol. Helv.* **68**, 247–280.

Simpson, C. & Schmid, S. M. 1983. An evaluation of criteria to deduce the sense of movement in sheared rocks. *Bull. geol. Soc. Am.* **94**, 1281–1288.

Soper, N. J. & Barber, A. J. 1982. A model for the deep structure of the Moine thrust zone. *J. geol. Soc. Lond.* **139**, 127–138.

Soper, N. J. & Wilkinson, P. 1975. The Moine Thrust and Moine Nappe at Loch Eriboll, Sutherland. *Scott. J. Geol.* **4**, 339–359.

Starkey, J. 1970. A computer programme to prepare orientation diagrams. In: *Experimental and Natural Rock Deformation* (edited by Paulitsch, P.). Springer Verlag, Berlin, 51–74.

Tullis, J. A., Christie, J. M. & Griggs, D. T. 1973. Microstructures and preferred orientations of experimentally deformed quartzites. *Bull. geol. Soc. Am.* **84**, 297–314.

Twiss, R. J. 1977. Theory and applicability of a recrystallised grain size palaeopiezometer. *Pure appl. Geophys.* **115**, 227–244.

Weathers, M. S., Bird, J. M., Cooper, R. F. & Kohlstedt, D. C. 1979. Differential stress determined from deformation induced microstructures of the Moine Thrust Zone. *J. geophys. Res.* **84**, 7495–7509.

White, S. H. 1979. Grain and sub-grain size variation across a mylonite zone. *Contr. Miner. Petrol.* **70**, 193–202.

White, S. H., Burrows, S. E., Carreras, J., Shaw, N. D. & Humphreys, F. J. 1980. On mylonites in ductile shear zones. *J. Struct. Geol.* **2**, 175–187.

White, S. H., Evans, D. J. & Zhong, D. L. 1982. Fault rocks of the Moine Thrust Zone, microstructures and textures of selected mylonites. *Textures Microstruct.* **5**, 33–61.